

Chapter 9

Graph Enumeration

9.1 Burnside-Pólya Counting

9.2 Burnside's Lemma

9.3 Counting Small Simple Graphs

9.4 Partitions of Integers

9.5 Calculating a Cycle Index

9.6 General Graphs and Digraphs

Pólya showed how the algebraic theorem called Burnside's Lemma could be augmented to count graph isomorphism types. A couple of decades after Pólya, Harary launched an extensive program of developing additional augmentations. The present chapter presents the basics of the method and should how it can be used to count the isomorphism types of various graph objects, including simple graphs, general graphs, and digraphs.

9.1 BURNSIDE-PÓLYA COUNTING

This section presents a way to algebraize a problem of counting equivalence classes under geometric or other symmetries, by representing the symmetries as a collection of permutations. Proof that the technique works is deferred to §9.2.

REVIEW FROM §1.6:

- A *permutation of a set* S is a one-to-one, onto function from S to itself.
- **Cor 1.6.4.** Every permutation of a finite set S can be represented as the composition of disjoint cycles of elements of S .

FROM APPENDIX A2:

- An algebraic system $\langle U, \star \rangle$ is called a **group** if it has the following properties:
 - the operation \star is associative.
 - there is an identity element.
 - every element of U has an inverse.

Example 9.1.1: Suppose that each square of a 2×2 -checkerboard is to be colored black or white. Then, since the number of squares is 4 and the number of colors is at most 2, the number of possible colorings is $2^4 = 16$. These 16 colorings are partitioned into 6 cells in Figure 9.1.1.

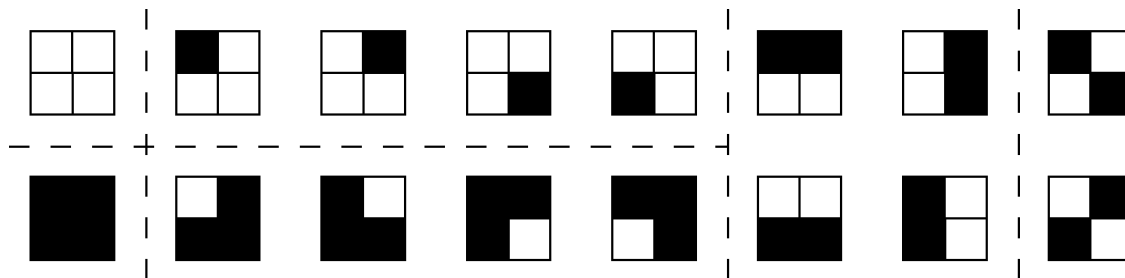


Fig 9.1.1 The sixteen 2×2 -checkerboards.

Broken lines partition the set of 16 checkerboards into six cells. Each such cell represents an *equivalence class* under a *geometric symmetry*. That is, any checkerboard within each cell could be obtained from any other checkerboard in the cell by one of the clockwise rotations in the set

$$G = \{0^\circ, 90^\circ, 180^\circ, 270^\circ\}$$

Also, there are no two boards in different cells that are related by one of the clockwise rotations. Thus, up to rotational symmetry, the number of colorings is 6.

The set of four rotations under composition forms a *group*. Having a group of symmetries is a highly significant feature in counting problems.

Counting equivalence classes of colorings can be easily done, for 2 colors on a 2×2 board, simply by drawing all cases and organizing them into equivalence classes, as in Figure 9.1.1. However, what if there were 5 possible colors and the board was 4×4 , as in Figure 9.1.2?

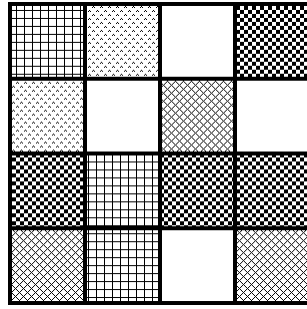


Fig 9.1.2 A 5-colored 4×4 -checkerboard.

Since there are 16^5 such 5-colorings, and since the maximum size of an equivalence class is 4, the number of equivalence classes would be at least

$$\frac{5^{16}}{4}$$

The remarkable counting method known as *Burnside-Pólya counting* is used for such enumeration problems, to obtain the exact number of classes.

Permutations on Discrete Sets

The set-up for Burnside-Pólya counting under a group of symmetries is to represent the objects of the symmetries as a discrete set and to represent each symmetry as a permutation.

DEF: A closed non-empty collection P of permutations on a set Y of objects that forms a group under the operation of composition is called a **permutation group**. The combined structure may be denoted $\mathcal{P} = [P : Y]$. It is often denoted P when the set Y of objects is understood from context.

Remark: The phrase *permutation group* usually refers to a non-commutative group, even though some of our early examples are commutative.

Example 9.1.1, cont.: The objects in the problem of counting checkerboards are the individual squares of the checkerboard. Each of the four squares is assigned a number, starting with the number 1 in the upper right, and proceeding clockwise in assigning 2, 3, and 4, as shown in Figure 9.1.3.

1	2
4	3

Fig 9.1.3 Numbering the squares of a checkerboard.

The four rotational symmetries of the group G that acts on the 2×2 checkerboard can be represented as permutations of the numbers assigned to its squares, as shown in the second column of Table 9.1.1.

Table 9.1.1 Algebraizing checkerboard symmetry.

rotation	permutation
0°	$(1)(2)(3)(4)$
90°	$(1\ 2\ 3\ 4)$
$180^\circ = 2 \times 90^\circ$	$(1\ 2\ 3\ 4)^2 = (1\ 3)(2\ 4)$
$270^\circ = 3 \times 90^\circ$	$(1\ 2\ 3\ 4)^3 = (1\ 4\ 3\ 2)$

It is easily verified that this collection of permutations satisfies the group axioms. We may observe that it is commutative.

Cyclic Permutations

DEF: A permutation on a set Y whose representation in disjoint cycle form has only one cycle containing more than one element of Y is called a ***cyclic permutation***.

- The number of elements in that one cycle is called the ***length of that cycle***. Also, a cycle of length k is called a k -cycle.

Proposition 9.1.1. Let $n \in \mathbb{Z}^+$, and let

$$\alpha = (1\ 2\ \dots\ n)$$

Then for $j = 1, \dots, n-1$ and for $r = 1, \dots, n$, we have

$$\alpha^j(r) = \begin{cases} r + j & \text{if } r + j \leq n \\ r + j \bmod n & \text{otherwise} \end{cases}$$

Proof: This is provable by induction on the power j . It is clearly true for $j = 1$. The inductive hypothesis is that

$$\alpha^{j-1}(r) = \begin{cases} r + j - 1 & \text{if } r + j - 1 \leq n \\ r + j - 1 \bmod n & \text{otherwise} \end{cases}$$

The inductive step is that

$$\begin{aligned} \alpha^j(r) &= \alpha^1 \alpha^{j-1}(r) = \begin{cases} \alpha^1(r + j - 1) & \text{if } r + j - 1 \leq n \\ \alpha^1(r + j - 1 \bmod n) & \text{otherwise} \end{cases} \\ &= \begin{cases} r + j & \text{if } r + j \leq n \\ r + j \bmod n & \text{otherwise} \end{cases} \quad \diamond \end{aligned}$$

Corollary 9.1.2. *Let p be a prime number, and let the permutation α be the p -cycle $(1 \ 2 \ \dots \ p)$. Then for $j = 1, \dots, p - 1$, the permutation*

$$\alpha^j = (1 \ 2 \ \dots \ p)^j$$

in the group \mathbb{Z}_p is a p -cycle.

Proof: It is sufficient to show that each two elements of the sequence

$$1 \ \alpha^j(1) \ \alpha^{2j}(1) \ \dots \ \alpha^{(p-1)j}(1) \quad (9.1.1)$$

are distinct. Suppose, to the contrary, that

$$\alpha^{uj}(1) = \alpha^{vj}(1)$$

for some pair u and v such that $1 \leq u, v \leq p - 1$. Then, by Proposition 9.1.1, we have

$$uj + 1 \equiv vj + 1 \pmod{p}$$

It follows that

$$p \mid uj - vj$$

and in turn, since p is prime, that

$$p \mid j \quad \text{or} \quad p \mid (u - v)$$

Since $1 \leq j \leq p - 1$, it follows that

$$p \mid (u - v)$$

Since $0 \leq u, v \leq p - 1$, it now follows that

$$u = v$$

Hence, by the pigeonhole principle, the sequence (9.1.1) contains all of the numbers $1, \dots, p$. Accordingly, we have

$$\alpha^j = (1 \ 1 + j \ 1 + 2j \ \cdots \ 1 + (p - 1)j) \quad (9.1.2)$$

That is, the permutation α^j is a p -cycle. \diamond

Example 9.1.2: Let α be the 5-cycle $(1 \ 2 \ 3 \ 4 \ 5)$. Then we have

$$\alpha^3 = (1 \ 4 \ 2 \ 5 \ 3) \quad \text{and} \quad \alpha^4 = (1 \ 5 \ 4 \ 3 \ 2)$$

Example 9.1.3: However, if α is the n -cycle $(1 \ 2 \ \cdots \ n)$ and the number n is not prime, then some of the permutations α^j are not cyclic. For instance, for $\alpha = (1 \ 2 \ 3 \ 4)$, we have

$$\alpha^2 = (1 \ 3)(2 \ 4)$$

as previously observed in Table 9.1.1.

Cyclic Permutation Groups

Table 9.1.2 generalizes the group of Table 9.1.1 to a permutation group on the set $\{1, 2, \dots, n\}$. Geometrically, visualize the numbers as equally spaced in cyclic order $1, 2, \dots, n$ around the unit circle in the xy -plane.

Table 9.1.2 The cyclic permutation group \mathbb{Z}_n .

rotation	permutation
0	$(1)(2) \cdots (n)$
$\frac{2\pi}{n}$	$(1\ 2\ \cdots\ n)$
$2 \cdot \frac{2\pi}{n}$	$(1\ 2\ \cdots\ n)^2$
\dots	\dots
$(n-1) \cdot \frac{2\pi}{n}$	$(1\ 2\ \cdots\ n)^{n-1}$

DEF: The group of permutations in Table 9.1.2 is called a **cyclic permutation group** on the set $\{1, 2, \dots, n\}$. It can be denoted $[\mathbb{Z}_n : [1 : n]]$, but is more usually denoted, simply, \mathbb{Z}_n .

Prop 9.1.3. *The permutation group \mathbb{Z}_n is commutative, for $n \in \mathbb{Z}^+$.*

Proof: Let $\alpha = (1\ 2\ \cdots\ n)$. Then, as indicated by Table 9.1.2, any two perms in \mathbb{Z}_n could be represented

in the forms α^r and α^s . Then

$$\alpha^r \alpha^s = \alpha^{r+s} = \alpha^{s+r} = \alpha^s \alpha^r \quad \diamond$$

Corollary 9.1.2 establishes that if n is prime, then every permutation in the cyclic permutation group Z_n is cyclic. However, when $n = 4$, which is not prime, as first noted in Table 9.1.1, we have

$$(1 \ 2 \ 3 \ 4)^2 = (1 \ 3)(2 \ 4)$$

That is, the permutations in a cyclic permutation group need not all be cyclic permutations. The next proposition sharpens this observation.

Prop 9.1.4. *Let $\alpha = (1 \ 2 \ \dots \ n)$ be an n -cycle in Z_n . Then for $j = 1, \dots, n-1$, the permutation α^j has $\gcd(j, n)$ cycles, each of length*

$$\frac{n}{\gcd(j, n)}$$

Proof: For an arbitrary object $k \in [1 : n]$, we observe that all the objects in the cycle containing k must lie in the sequence

$$k \ \alpha^j(k) \ \alpha^{2j}(k) \ \dots \ \alpha^{(n-1)j/\gcd(j,n)}(k) \quad (9.1.3)$$

This is because the next element in that sequence would be

$$\alpha^{nj/\gcd(j,n)}(k) = (\alpha^n)^{j/\gcd(j,n)}(k) = k$$

which holds because α^n is the identity permutation. Thus, the maximum length of a cycle of the permutation α^j is

$$\frac{n}{\gcd(j, n)}$$

We next assert that the elements of the sequence (9.1.3) are mutually distinct. To see this, suppose that

$$1 \leq u \leq v \leq \frac{n-1}{\gcd(j, n)} \quad (9.1.4)$$

and that $\alpha^{uj}(k) = \alpha^{vj}(k)$. Then, by Proposition 9.1.1, we have

$$uj + k \equiv vj + k \pmod{n}$$

It follows that

$$n \mid vj - uj$$

and, in turn, that $\frac{n}{\gcd(j, n)}$ divides $v - u$. By (9.1.4), it now follows that $u = v$. Thus, the minimum length of a cycle in α^j is

$$\frac{n}{\gcd(j, n)}$$

It follows that every cycle of the permutation α^j is of that length. \diamond

Cor 9.1.5. *Let $\alpha = (1 \ 2 \ \cdots \ n)$ be a permutation in \mathbb{Z}_n . Then for $j = 1, \dots, n-1$, the permutation α^j is cyclic if and only if $j \perp n$. \diamond*

Example 9.1.4: Let $\alpha = (1 \ 2 \ \cdots \ 12)$ in the cyclic permutation group \mathbb{Z}_{12} . Since

$$\gcd(8, 12) = 4 \quad \text{and} \quad \frac{12}{4} = 3$$

Proposition 9.1.4 implies that the permutation α^8 has four 3-cycles. In fact,

$$\alpha^8 = (1 \ 9 \ 5)(2 \ 10 \ 6)(3 \ 11 \ 7)(4 \ 12 \ 8)$$

Example 9.1.5: Let $\alpha = (1 \ 2 \ \cdots \ 10)$ in \mathbb{Z}_{10} . Since

$$\gcd(3, 10) = 1 \quad \text{and} \quad \frac{10}{1} = 10$$

Proposition 9.1.4 implies that α^3 has one 10-cycle. In fact,

$$\alpha^3 = (1 \ 4 \ 7 \ 10 \ 3 \ 6 \ 9 \ 2 \ 5 \ 8)$$

Cycle Structure of a Permutation

After representing the context of the counting by a permutation group, we can turn to the main calculation of Burnside-Pólya counting, which is to determine a polynomial called the *cycle index* for that group.

TERMINOLOGY: A *monomial* is a polynomial with only one term.

DEF: Let π be a permutation on a set of n objects. Then the **cycle structure** of π is the n -variable monomial

$$\zeta(\pi) = \prod_{i=j}^n t_j^{r_j} = t_1^{r_1} t_2^{r_2} \cdots t_n^{r_n}$$

where t_j is a formal variable, and where r_j is the number of j -cycles in the disjoint cycle form of π .

Example 9.1.1, continued: Table 9.1.3 extends Table 9.1.1 by adding a column with the cycle structures of the permutations and a bottom row to be explained below.

Table 9.1.3 Cycle structures of the permutations.

symmetry	permutation	cycle structure
0°	$(1)(2)(3)(4)$	t_1^4
90°	$(1\ 2\ 3\ 4)$	t_4
180°	$(1\ 3)(2\ 4)$	t_2^2
270°	$(1\ 4\ 3\ 2)$	t_4
cycle index		$= \frac{1}{4} (t_1^4 + t_2^2 + 2t_4)$

In Table 9.1.3, the perm $(1)(2)(3)(4)$ has the cycle structure t_1^4 , because it has four 1-cycles and no other cycles. The perm $(1\ 3)(2\ 4)$ has structure t_2^2 , because it has two 2-cycles and no other cycles. The perms $(1\ 2\ 3\ 4)$ and $(1\ 4\ 3\ 2)$ both have cycle structure t_4 , because they have one 4-cycle and no other cycles.

DEF: Let $\mathcal{P} = [P : Y]$ be a permutation group on a set of n objects. Then the **cycle index** of \mathcal{P} is the polynomial

$$Z_{\mathcal{P}}(t_1, \dots, t_n) = \frac{1}{|P|} \sum_{\pi \in P} \zeta(\pi)$$

where $\zeta(\pi)$ is the cycle structure of π .

Example 9.1.1, continued: Observe that the cycle index for the group of symmetries on the checkerboard is recorded at the bottom of Table 9.1.3.

Evaluating the Cycle Index

After the cycle index polynomial is calculated, the final step of Burnside-Pólya counting is to evaluate the cycle index, by making a substitution for each of its variables t_1, \dots, t_n . If the objective is simply to obtain the total number of colorings under the symmetries, then substitute the cardinality of the color set for every variable t_j .

Example 9.1.1, continued: The bottom line of Table 9.1.3 contains the cycle index for the permutation group acting on the 2×2 -checkerboard.

$$Z_{\mathbb{Z}_4}(t_1, \dots, t_4) = \frac{1}{4} (t_1^4 + t_2^2 + 2t_4)$$

The number of black-white 2×2 checkerboards is obtained by substituting 2 for each of the variables t_1, \dots, t_4 . Thus, the number of boards is

$$\frac{1}{4} (2^4 + 2^2 + 2 \cdot 2) = \frac{1}{4} (16 + 4 + 4) = 6$$

DEF: Substituting the polynomial $c_1^j + \cdots + c_k^j$ for the variable t_j , for $j = 1, \dots, n$, into the cycle index is called **Pólya substitution** for k colors. The resulting polynomial in the indeterminates c_1, \dots, c_k is called a **Pólya inventory**.

The objective of Pólya substitution is to obtain a more detailed enumeration. It is frequently calculated with the aid of a table.

Example 9.1.1, continued: Table 9.1.4 calculates a Pólya inventory for the black-white 2×2 -checkerboards. The mnemonic indeterminates b (for *black*) and w (for *white*) are used in place of the generic c_1 and c_2 .

Table 9.1.4 Pólya inventory for 2×2 -checkerboards.

cycle structure	subst	b^4	b^3w	b^2w^2	bw^3	w^4
t_1^4	$(b + w)^4$	1	4	6	4	1
t_2^2	$(b^2 + w^2)^2$	1	0	2	0	1
$2t_4$	$2(b^4 + w^4)$	2	0	0	0	2
sum		4	4	8	4	4
$\div 4$		1	1	2	1	1

In each row of the table, the entry in the first column is one of the terms of the cycle index polynomial, and the entry in the second column is the result of Pólya substitution, unexpanded. The remaining columns show the expansion.

Thus, the Pólya inventory polynomial is

$$b^4 + b^3w + 2b^2w^2 + bw^3 + w^4$$

With the monomial b^jw^{4-j} signifying j black squares and $4-j$ white squares, then this calculation agrees with Figure 9.1.1.

Example 9.1.6: If the number of colors for the 2×2 -board is increased to 3, then the number of boards is

$$\frac{1}{4} (3^4 + 3^2 + 2 \cdot 3) = \frac{1}{4} (81 + 9 + 6) = 24$$

If only one color is actually used, then there are 3 choices of a color. If exactly two colors are used, there are $\binom{3}{2} = 3$ choices of two colors and then 4 patterns (from Example 9.1.5) possible for each such choice, for a subtotal of $3 \cdot 4 = 12$. If all three colors are used, there are 3 choices of the color that is used on two squares and three possible patterns with those colors, up to rotation, as shown in Figure 9.1.4, for a subtotal of 9. The sum of the three subtotals 3, 12, and 9 is 24, thereby confirming the Burnside-Pólya calculation.

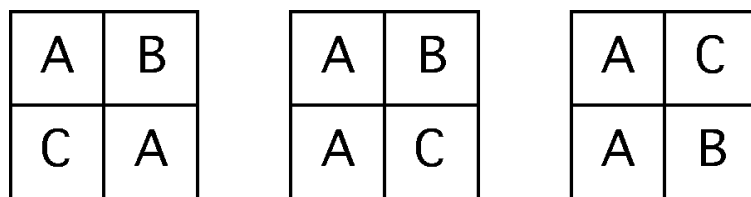


Fig 9.1.4 The three 3-color patterns, up to rotation.

Reflections

In addition to the four rotations on a checkerboard, there are also four reflections. If they are included with the four rotations, there would be a perm group of cardinality 8. For 2-coloring the 2×2 -board of Figure 9.1.3,

1	2
4	3

there would be the following additional permutations and cycle structures in the cycle index.

Table 9.1.5 Cycle structures of the four reflections.

reflection	permutation	cycle structure
thru x – axis	$(1\ 4)(2\ 3)$	t_2^2
thru y – axis	$(1\ 2)(3\ 4)$	t_2^2
NE diagonal	$(2)(4)(1\ 3)$	$t_1^2 t_2$
SE diagonal	$(1)(3)(2\ 4)$	$t_1^2 t_2$

To generalize from Table 9.1.5 to reflections on a larger set of objects, we model the set $\{1, 2, \dots, n\}$ as points evenly spaced around the unit circle. There are n possible reflections of the plane through a line through

the origin that map this set of points bijectively onto itself. Each corresponds to a permutation of the set of numbers, as illustrated in Figure 9.1.5. Each cycle in each such permutation is either a 1-cycle or a 2-cycle.

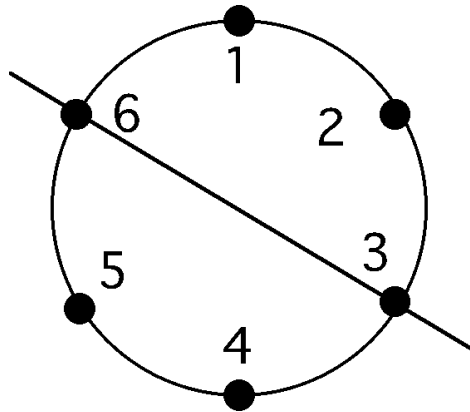


Fig 9.1.5 The reflection $(1\ 5)(2\ 4)(3)(6)$.

It is natural to regard the cyclic permutation

$$\alpha = (1\ 2\ \cdots\ n)$$

as the *principal rotation* on the unit circle model of $[1 : n]$. Suppose that we similarly regard the permutation

$$\beta(i) = n + 1 - i$$

as the *principal reflection* on $[1 : n]$. We observe that β corresponds to a reflection of the unit circle through a line through the origin that bisects the arc between the points numbered 1 and n . If n is odd, this line also passes thru the point numbered $\frac{n+1}{2}$. If n is even, it bisects the arc between the points numbered $\frac{n}{2}$ and $\frac{n}{2} + 1$. In the immediate context, we call this line the β -bisector.

Remark: We observe that the composition permutation

$$\alpha^j \beta(i) = \alpha^j(n+1-i) = \begin{cases} 1+j-i & \text{if } j \geq i \\ n+1+j-i & \text{otherwise} \end{cases}$$

represents reflection through the circle bisector obtained by rotating the β -bisector $\frac{j\pi}{n}$ radians clockwise.

Example 9.1.7: The reflection $(1\ 5)(2\ 4)(3)(6)$ depicted in Figure 9.1.5 is $\alpha^5\beta$.

Dihedral Permutation Groups

The composition of any two reflections on the unit circle model of

$$\{1, 2, \dots, n\}$$

is a rotation, and the composition of a rotation and a reflection is a reflection. Accordingly, the union of the sets of rotations and reflections on $\{1, 2, \dots, n\}$ is closed under composition. Thus, it forms a permutation group.

Example 9.1.8: This composition of reflections

$$(1\ 5)(2\ 4)(3)(6) \circ (1\ 4)(2\ 3)(5\ 6)$$

is the rotation

$$(1\ 6\ 5\ 4\ 3\ 2)$$

DEF: The permutation group

$$\{\alpha^j \mid j \in [1 : n]\} \cup \{\alpha^j \beta \mid j \in [1 : n]\}$$

is denoted \mathbb{D}_n and called the **dihedral group** on the cyclic set $\{1, 2, \dots, n\}$.

Example 9.1.9: Thus, the dihedral group \mathbb{D}_4 is given in Table 9.1.6, which is formed from the union of the rotations of Table 9.1.3 and the reflections of Table 9.1.5.

Table 9.1.6 The dihedral group \mathbb{D}_4 .

symmetry	permutation	cycle structure
0°	$(1)(2)(3)(4)$	t_1^4
90°	$(1\ 2\ 3\ 4)$	t_4
180°	$(1\ 3)(2\ 4)$	t_2^2
270°	$(1\ 4\ 3\ 2)$	t_4
x – axis	$(1\ 4)(2\ 3)$	t_2^2
y – axis	$(1\ 2)(3\ 4)$	t_2^2
SE diag	$(1)(3)(2\ 4)$	$t_1^2 t_2$
NE diag	$(2)(4)(1\ 3)$	$t_1^2 t_2$

$$\text{cycle index } \mathcal{Z}_{\mathbb{D}_4} : \quad \frac{1}{8} (t_1^4 + 2t_1 t_2 + 3t_2^2 + 2t_4)$$

Using the cycle index of \mathbb{D}_4 on its bottom line, one can calculate that the corresponding number of colorings would be

$$\begin{aligned} \mathcal{Z}_{\mathbb{D}_4}(2, \dots, 2) &= \frac{1}{8} (2^4 + 2 \cdot 2^2 \cdot 2 + 3 \cdot 2^2 + 2 \cdot 2) \\ &= \frac{1}{8} (16 + 16 + 12 + 4) \\ &= \frac{48}{8} = 6 \end{aligned}$$

This corresponds to the observation that the partition of 2-colorings in Figure 9.1.1 corresponds to dihedral symmetry as well as to pure rotational symmetry. By way of contrast, the middle and rightmost 3-coloring patterns of Figure 9.1.4 are related by reflection. Thus, one expects, as now calculated, that there would be fewer dihedral classes than the 24 classes of colorings (under rotation) that were counted in Example 9.1.6.

$$\begin{aligned} Z_{\mathbb{D}_4}(3, \dots, 3) &= \frac{1}{8} (3^4 + 2 \cdot 3^2 \cdot 3 + 3 \cdot 3^2 + 2 \cdot 3) \\ &= \frac{1}{8} (81 + 54 + 27 + 6) \\ &= \frac{168}{8} = 21 \end{aligned}$$

Larger Sets of Permuted Objects

When the same two groups of four or eight geometric symmetries act on larger checkerboards, the cycle structures of the permutations change, even though the terminology is preserved.

Example 9.1.10: The 3×3 -checkerboard of Figure 9.1.6 has the following table of permutations and cycle structures for its dihedral symmetry group.

1	2	3
8	9	4
7	6	5

Fig 9.1.6 The 3×3 -checkerboard.

Table 9.1.7 Symmetries on the 3×3 -checkerboard.

symmetry	permutation	cycle structure
0°	$(1)(2)\cdots(9)$	t_1^9
90°	$(9)(1\ 3\ 5\ 7)(2\ 4\ 6\ 8)$	$t_1 t_4^2$
180°	$(5)(1\ 5)(2\ 6)(3\ 7)(4\ 8)$	$t_1 t_2^4$
270°	$(9)(1\ 7\ 5\ 3)(2\ 8\ 6\ 4)$	$t_1 t_4^2$
x - axis	$(4)(8)(9)(1\ 7)(2\ 6)(3\ 5)$	$t_1^3 t_2^3$
y - axis	$(2)(6)(9)(1\ 3)(4\ 8)(5\ 7)$	$t_1^3 t_2^3$
SE diag	$(1)(5)(9)(2\ 8)(3\ 7)(4\ 6)$	$t_1^3 t_2^3$
NE diag	$(3)(7)(9)(1\ 5)(2\ 4)(6\ 8)$	$t_1^3 t_2^3$

$$\text{cycle index} = \frac{1}{8} (t_1^9 + t_1 t_4^4 + 2t_1 t_4^2 + 4t_1^3 t_2^3)$$

Thus, as the number of ways to color the 3×3 checkerboard with at most 2 colors, Burnside-Pólya counting gives

$$\frac{1}{8} (2^9 + 2 \cdot 2^4 + 2 \cdot 2 \cdot 2^2 + 4 \cdot 2^3 \cdot 2^3) = 102$$

9.2 BURNSIDE'S LEMMA

The mathematical principle that underlies the calculations of §9.1 has commonly been called *Burnside's Lemma*, after its appearance in Burnside's influential monograph [Burn1911].

DEF: Let $\mathcal{P} = [P : Y]$ be a permutation group, and let $y \in Y$. The **orbit** of the object y under the action of P is the set $\{\pi(y) \mid \pi \in P\}$.

With the benefit of this definition, we may say that Burnside's Lemma counts orbits.

Proposition 9.2.1. *Let $\mathcal{P} = [P : Y]$ be a permutation group. Then being co-orbital is an equivalence relation.*

Proof: The identity permutation maps each object to itself, so each object is in its own orbit. If $\pi(y) = y'$, then $\pi^{-1}(y') = y$, so the relation is symmetric. If $\pi(y) = y'$ and $\pi'(y') = y''$, then $(\pi' \circ \pi)(y) = y''$, so the relation is transitive. \diamond

Orbits

Given a permutation group $\mathcal{P} = [P : Y]$, the orbit of an object y can be computed from a listing of the disjoint cycle form for every permutation $\pi \in P$. Quite simply, the orbit of y is the set of objects that appear in the same

cycle as y in any of the permutations π . More efficiently to compute, the orbit of y is also the set of objects that appear immediately after y in some permutation of the group.

Example 9.2.1: When the group of 4 rotations acts on the set of squares of the 2×2 -checkerboard, then all 4 squares are in the same orbit.

1	2
4	3

rotation	permutation
0°	$(1)(2)(3)(4)$
90°	$(1\ 2\ 3\ 4)$
180°	$(1\ 3)(2\ 4)$
270°	$(1\ 4\ 3\ 2)$

However, when the group of 4 rotations acts on the set of 16 colorings of the board with at most two colors, there are 6 orbits, as indicated in Figure 9.1.1. In this particular example, they happen to be identifiable with the cells of the 90° rotation, as illustrated in Figure 9.2.1.

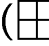
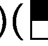
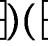
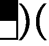
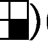





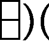





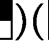
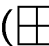


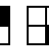

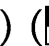



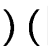






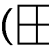


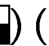
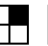






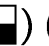






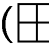


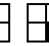
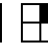
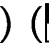



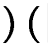




rotation	permutation
0°	() () () () () () () () () () () () () () () () ()
90°	() (   ) (   ) ( ) (   ) ()
180°	() ( ) ( ) ( ) ( ) ( ) ( ) ( ) ( ) ()
270°	() (   ) ( ) ( ) (   ) ()

Fig 9.2.1 Permutations of the colored 2×2 boards.

Remark: Although the next lemma mentions orbits of perm groups, it is really a fact about set partitions.

Lemma 9.2.2. *Let $\mathcal{P} = [P : Y]$ be a permutation group with n orbits. Then*

$$\sum_{y \in Y} \frac{1}{|\text{orbit}(y)|} = n \quad (9.2.1)$$

Proof: Suppose that Y_1, \dots, Y_n are the orbits. Since the orbits Y_j partition Y , it follows that

$$\begin{aligned} \sum_{y \in Y} \frac{1}{|\text{orbit}(y)|} &= \sum_{j=1}^n \sum_{y \in Y_j} \frac{1}{|\text{orbit}(y)|} \\ &= \sum_{j=1}^n \sum_{y \in Y_j} \frac{1}{|Y_j|} \\ &= \sum_{j=1}^n \frac{1}{|Y_j|} \sum_{y \in Y_j} 1 = \sum_{j=1}^n \frac{1}{|Y_j|} |Y_j| \\ &= \sum_{j=1}^n 1 = n \quad \diamond \end{aligned}$$

Example 9.2.2: The left side of Equation (9.2.1) is the sum of the reciprocals of the sizes of the cells in a partition. The partition depicted at the left of Figure 9.2.2 has three cells. When the objects in the cells are converted to the reciprocals of the cell sizes, as on the right, then the sum

of the fractions within each cell must equal 1. Thus, the sum of all the reciprocals must equal the number of cells, as on the right side of the equation in Lemma 9.2.2.

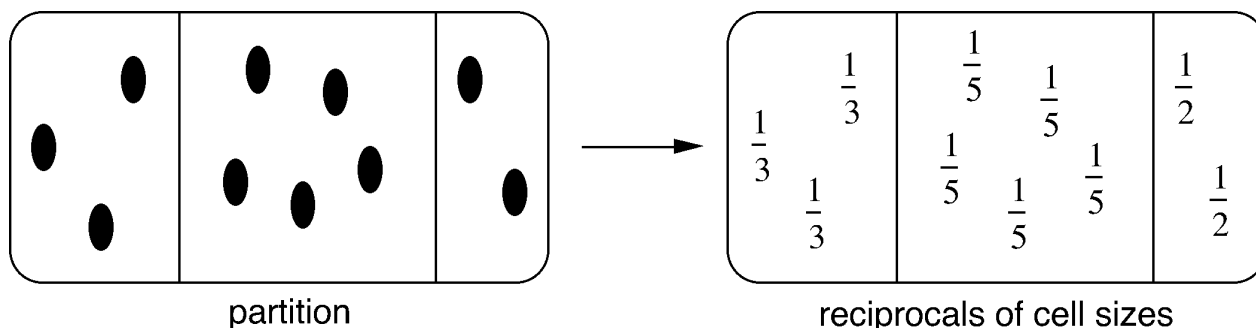


Fig 9.2.2 Reciprocals of cell sizes of a partition.

Induced Actions on Colorings

Pólya's main contribution to the counting method was to discover a relationship between the cycle index of a permutation group action on a set Y and the number of orbits *induced on* the colorings of Y .

DEF: A **k -coloring** of a set Y is a mapping f from Y onto the set

$$\{1, 2, \dots, k\}$$

TERMINOLOGY: The value $f(y)$ is called the **color** of the object y . Often the names or initials of actual colors, such as black and white, are used in place of integer values.

DEF: A **$(\leq k)$ -coloring** of a set Y is a coloring that uses k or *fewer* colors, formally a mapping f from Y onto any set $\{1, 2, \dots, t\}$ with $t \leq k$.

NOTATION: The set of all $(\leq k)$ -colorings of the elements of a set Y is denoted $Col_k(Y)$.

Example 9.2.3: Figure 9.2.3, a copy of Figure 9.1.1, represents all the (≤ 2) -colorings of $\{1, 2, 3, 4\}$ as 2×2 -checkerboards.

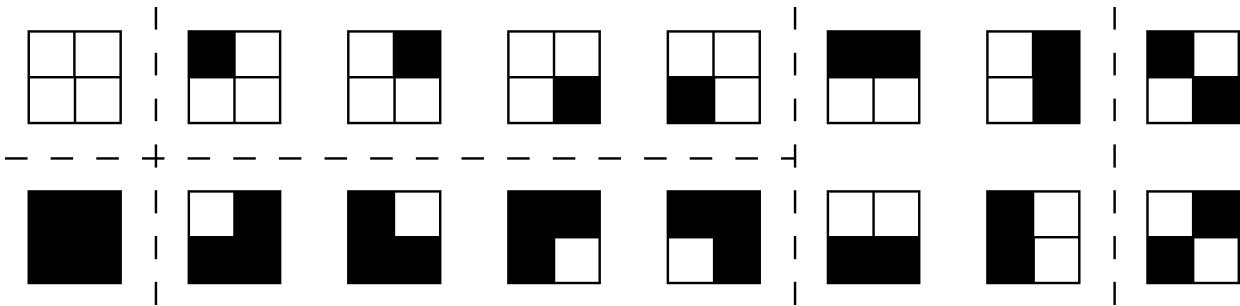


Fig 9.2.3 The 16 2×2 -checkerboards.

Prop 9.2.3. Let Y be a set. Then $|Col_k(Y)| = k^{|Y|}$.

Proof: This is a direct application of the Rule of Product (see §0.4). \diamond

Example 9.2.3, cont.: There are 16 (≤ 2) -colorings of the set $\{1, 2, 3, 4\}$, as shown in Figure 9.2.3.

DEF: Let $\mathcal{P} = [P : Y]$ be a perm group acting on a set Y , and let f and g be $(\leq k)$ -colorings of the objects in Y .

- Then the coloring f is \mathcal{P} -**equivalent** to the coloring g if there is a permutation $\pi \in P$ such that $g = f\pi$, that is, if for every object $y \in Y$, the color $g(y)$ is the same as the color $f(\pi(y))$.
- The mapping $f \mapsto f\pi$ is a permutation on the colorings, called the **induced action** of π on the set of

colorings. The notation $[P : Col_k(Y)]$ distinguishes the permutation group of such induced actions from the group $[P : Y]$.

Example 9.2.3, cont.: The 2-coloring

$$f : \quad 1 \mapsto b \quad 2 \mapsto w \quad 3 \mapsto w \quad 4 \mapsto w$$

is \mathbb{Z}_4 -equivalent to the 2-coloring

$$g : \quad 1 \mapsto w \quad 2 \mapsto b \quad 3 \mapsto w \quad 4 \mapsto w$$

under the permutation

$$\pi : \quad (1 \quad 2 \quad 3 \quad 4)$$

This is formally why the coloring with its one black square in the upper left corner of a 2×2 -checkerboard, represented in this example as the mapping f , is equivalent to the coloring with its one black square at the upper right, represented by the mapping g , under the 90° rotation, represented by the permutation π .

Fixed Points

DEF: Let $\mathcal{P} = [P : Y]$ be a permutation group, and let $\pi \in P$. A **fixed point** of π is an object $y \in Y$ such that $\pi(y) = y$.

NOTATION: $Fix(\pi)$ denotes the set of all fixed points of the permutation π .

Remark: The fixed point set $Fix(\pi)$ comprises the objects that lie in the 1-cycles of π .

Example 9.2.3, cont.: The number of fixed points of each of the four rotations is different for different sets on which the rotation group acts.

rotation	# fixed pts in $\{1, 2, 3, 4\}$	# fixed pts in 2×2 – colorings
0°	4	16
90°	0	2
180°	0	4
270°	0	2
total # fixed pts	4	24

Stabilizers

DEF: Let $\mathcal{P} = [P : Y]$ be a perm group, and let $y \in Y$. The *stabilizer* of y is the subset

$$Stab(y) = \{\pi \in P \mid \pi(y) = y\}$$

of the permutation group P .

Remark: Clearly, $Stab(y)$ is a subgroup of P . It is non-empty, since it contains the identity perm. It is closed under composition, because the composition of two perms that both fix object y must also fix the object y .

Remark: $Stab(y)$ can be constructed computationally as the set of all permutations in P in which the object y lies in a 1-cycle.

Example 9.2.4: When the rotation group \mathbb{Z}_4 acts on the set $\{1, 2, 3, 4\}$, the stabilizer $Stab(3)$ is the trivial subgroup

$$\{(1)(2)(3)(4)\}$$

Example 9.2.5: When the dihedral group \mathbb{D}_4 acts on the set $\{1, 2, 3, 4\}$, the stabilizer $Stab(3)$ is the subgroup

$$\{(1)(2)(3)(4), (1)(3)(2\ 4)\}$$

Example 9.2.6: Consider the rotation group \mathbb{Z}_4 acting on the set of 2×2 -checkerboards. The stabilizer of the board with four white squares is the entire group.

Lemma 9.2.4. *Let $\mathcal{P} = [P : Y]$ be a permutation group. Then*

$$\sum_{y \in Y} |Stab(y)| = \sum_{\pi \in P} |Fix(\pi)|$$

Proof: Consider a matrix M in which the rows are indexed by the objects of the set Y , and the columns indexed by the permutations in P , such that

$$M[y, \pi] = \begin{cases} 1 & \text{if } \pi(y) = y \\ 0 & \text{otherwise} \end{cases}$$

Then the sum of row y is $|Stab(y)|$ and the sum of column π is $|Fix(\pi)|$. This lemma simply asserts that the sum of the row sums of M equals the sum of its column sums, which is true of any matrix. \diamond

Lemma 9.2.5. *Let $\mathcal{P} = [P : Y]$ be a permutation group and $y \in Y$. Then*

$$|\text{Stab}(y)| = \frac{|P|}{|\text{orbit}(y)|}$$

Proof: Suppose that

$$\text{orbit}(y) = \{y = y_1, y_2, \dots, y_n\}$$

and that, for $j = 1, \dots, n$, we let P_j be the subset of permutations of P that maps object y to object y_j . Then the subsets

$$P_1, P_2, \dots, P_n$$

partition the permutation group P , and $P_1 = \text{Stab}(y)$.

For $j = 1, \dots, n$, let π_j be any permutation such that $\pi_j(y) = y_j$. Then the rule $\pi \mapsto \pi \circ \pi_j$ (composition with π_j) is a bijection from P_1 to P_j , which implies that

$$|P_j| = |P_1| = |\text{Stab}(y)|$$

for $j = 1, \dots, n$.

Since each of the n partition cells P_1, P_2, \dots, P_n of group P has cardinality $|\text{Stab}(y)|$, it follows that

$$n \cdot |\text{Stab}(y)| = |P|$$

But $n = |\text{orbit}(y)|$, which completes the proof. \diamond

Proof of Burnside's Lemma

Thm 9.2.6 [Burnside's Lemma]. Let $\mathcal{P} = [P : Y]$ be a permutation group with n orbits. Then

$$n = \frac{1}{|P|} \sum_{\pi \in P} |Fix(\pi)|$$

Proof: Lemmas 9.2.4, 9.2.5, and 9.2.2 establish the following chain of equalities, which proves Burnside's lemma.

$$\begin{aligned} \frac{1}{|P|} \sum_{\pi \in P} |Fix(\pi)| &= \frac{1}{|P|} \sum_{y \in Y} |Stab(y)| && \text{(Lemma 9.2.4)} \\ &= \frac{1}{|P|} \sum_{y \in Y} \frac{|P|}{|orbit(y)|} && \text{(Lemma 9.2.5)} \\ &= \frac{1}{|P|} |P| \sum_{y \in Y} \frac{1}{|orbit(y)|} \\ &= \sum_{y \in Y} \frac{1}{|orbit(y)|} = n && \text{(Lemma 9.2.2)} \quad \diamond \end{aligned}$$

Orbits of Induced Action on Colorings

In several examples of the preceding section, the orbits of an induced action

$$[P : Col_k(Y)]$$

on $(\leq k)$ -colorings were counted by substituting the number k of colors into the cycle index of the underlying action $[P : Y]$ on a set Y . The connection of this substitution into Burnside's Lemma — viz., that it counts the sum of the sizes of the fixed-point sets of the induced action — is now to be established.

Remark: The actions of \mathbb{Z}_n and \mathbb{D}_n on the set $\{1, \dots, n\}$ have only one orbit, because they both have a permutation in which a single cycle contains every object. One does not need Burnside's Lemma to count this one orbit.

NOTATION: If $p(x_1, \dots, x_n)$ is a multivariate polynomial, then $p(k, \dots, k)$ denotes the result of substituting the value k for every variable x_j .

Lemma 9.2.7. *Let $\mathcal{P} = [P : Y]$ be a permutation group, and let $\pi_Y \in P$, with induced action π_{CY} on the coloring set $Col_k(Y)$. Then the number of $(\leq k)$ -colorings of Y that are fixed by π_{CY} is given by*

$$|Fix(\pi_{CY})| = \zeta(\pi_Y)(k, \dots, k)$$

Proof: A $(\leq k)$ -coloring c is fixed by π_{CY} if and only if within each cycle of π_Y , all the objects are assigned the same color by c . Thus, there are k independent choices possible for each cycle of π_Y . Therefore,

$$|Fix(\pi_{CY})| = k^n$$

where n is the number of cycles in π_Y . But the number k^n is precisely the value of $\zeta(\pi_Y)(k, \dots, k)$. \diamond

Theorem 9.2.8. *Let $\mathcal{P} = [P : Y]$ be a permutation group. Then the number of orbits of $[P : Col_k(Y)]$ is*

$$\mathcal{Z}_{\mathcal{P}}(k, \dots, k)$$

Proof: Applying Burnside's lemma to the induced permutation group

$$[P : Col_k(Y)]$$

gives the number of orbits among the colorings as

$$\begin{aligned} \frac{1}{|P|} \sum_{\pi_{CY} \in PC} |Fix(\pi_{CY})| &= \frac{1}{|P|} \sum_{\pi_Y \in PY} \zeta(\pi_Y)(k, \dots, k) \quad (\text{Lemma 9.2.7}) \\ &= \mathcal{Z}_{\mathcal{P}}(k, \dots, k) \quad \diamond \end{aligned}$$

Pólya Inventory

As defined in §9.1, **Pólya substitution** means substituting the polynomial

$$c_1^j + \dots + c_k^j$$

for the variable t_j ($j = 1, \dots, n$) into the cycle index of a perm group $[P : Y]$. The resulting generating function in the indeterminates c_1, \dots, c_k is called a **Pólya inventory** for the color classes of the induced action $[P : Col_k(Y)]$.

Prop 9.2.9. *For any permutation group $\mathcal{P} = [P : Y]$, every term in the Pólya inventory for $[P : Col_k(Y)]$ has $|Y|$ as its degree.*

Proof: Let $\pi \in P_Y$ and let $\zeta(\pi) = t_1^{r_1} \cdots t_n^{r_n}$ be its cycle structure. Then, clearly,

$$\sum_{j=1}^n j \cdot r_j = |Y|$$

because π permutes the set Y and the sum is the total number of objects of Y over all the cycles of π . Substituting the polynomial $c_1^j + \cdots + c_k^j$ for a factor $t_j^{r_j}$ ($j = 1, \dots, n$) in $\zeta(\pi)$ contributes $j \cdot r_j$ to the degree of each corresponding term of the generating function. \diamond

Cor 9.2.10. For any permutation group $\mathcal{P} = [P : Y]$, the Pólya inventory for $[P : Col_k(Y)]$ is a sum

$$\sum_{s_1 + \cdots + s_k = |Y|} p_{s_1, \dots, s_k} c_1^{s_1} \cdots c_k^{s_k}$$

over the partitions of $|Y|$. \diamond

DEF: Let $\mathcal{P} = [P : Y]$ be a perm group. The **weight of a coloring** $f \in Col_k(Y)$ is a monomial $wt(f) = c_1^{s_1} \cdots c_k^{s_k}$ of degree $|Y|$ such that s_j is the number of objects of Y assigned color c_j , for $j = 1, \dots, k$. The **weight of a coloring orbit** is the weight of any coloring in that orbit.

Remark: The definition of the induced permutation action $[P : Col_k(Y)]$ implies that two colorings in the same orbit must have the same weight. Indeed, the weights are quite simply a mathematical device that enables us to inventory orbits according to some significant characteristic, such as the number of squares of a given color.

Theorem 9.2.11 [Pólya Inventory Theorem]. Let $\mathcal{P} = [P : Y]$ be a permutation group. Then every term

$$p_{s_1, \dots, s_k} c_1^{s_1} \cdots c_k^{s_k}$$

in a Pólya inventory for the induced action $[P : Col_k(Y)]$ has as its coefficient p_{s_1, \dots, s_k} the number of coloring orbits whose weight is $c_1^{s_1} \cdots c_k^{s_k}$.

Proof: A weighted form of Lemma 9.2.2 is that the coefficient of the weight $c_1^{s_1} \cdots c_k^{s_k}$ in the sum

$$\sum_{f \in Col_k(Y)} \frac{wt(f)}{|orbit(f)|}$$

is the number of orbits of weight $c_1^{s_1} \cdots c_k^{s_k}$. As before, it is really about partitions of sets. Similarly, a weighted version of Lemma 9.2.4 asserts that the sum over all permutations in $[P : Col_k(Y)]$ of the sums of the weights of their fixed-point sets equals the sum over all colorings $f \in Col_k(Y)$ of the products $wt(f) \cdot |Stab(f)|$. \diamond

Coloring Necklaces

We conclude this section with an application to a classic example, that of counting *necklaces*. Our model for an n -beaded necklace is a geometric conceptualization of the cycle graph C_n as a regular n -sided polygon, as illustrated in Figure 9.2.4. The numbering of the *beads* is used in specification of the permutations.

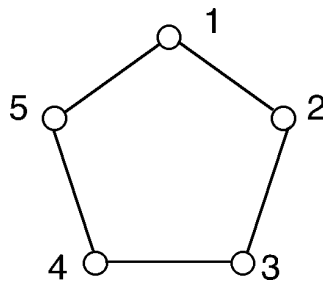


Fig 9.2.4 A 5-beaded necklace.

Example 9.2.7: Suppose that each bead is to be colored either black or white, and that two necklaces are indistinguishable (i.e., equivalent) if one can be obtained from the other by a rotation of the polygon. We model these symmetries by the cyclic permutation group \mathbb{Z}_5 , in which the clockwise rotation of $\frac{2\pi}{5}$ corresponds to the permutation

$$\alpha = (1 \ 2 \ 3 \ 4 \ 5)$$

The cycle structure of the identity permutation is t_1^5 . By Corollary 9.1.2, the cycle structure of the permutations

$$\alpha, \ \alpha^2, \ \alpha^3, \ \text{and} \ \alpha^4$$

is t_5 . Thus, the cycle index polynomial is

$$\mathcal{Z}_{\mathbb{Z}_5} = \frac{1}{5} (t_1^5 + 4t_5)$$

According to Theorem 9.2.8, the number of 2-colored, 5-beaded necklaces is

$$\frac{1}{5} (2^5 + 4 \cdot 2) = \frac{40}{5} = 8$$

Table 9.2.1 provides the corresponding Pólya inventory.

Table 9.2.1 Inventory for 5-beaded necklaces under cyclic symmetry.

cycle structure	subst	b^5	b^4w	b^3w^2	b^2w^3	bw^4	w^5
t_1^5	$(b+w)^5$	1	5	10	10	5	1
$4t_5$	$4(b^5+w^5)$	4	0	0	0	0	4
sum		5	5	10	10	5	5
$\div 5$		1	1	2	2	1	1

Figure 9.2.5 illustrates the eight necklaces.

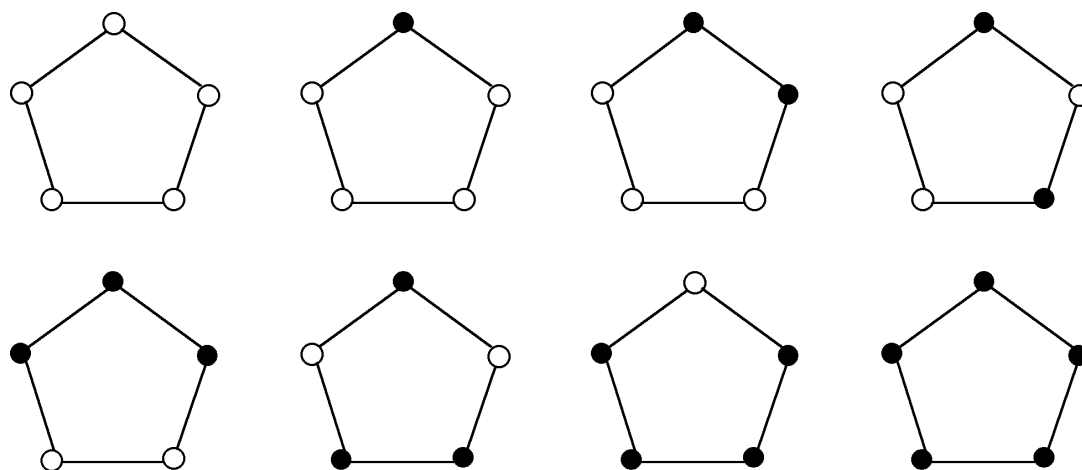


Fig 9.2.5 The eight 2-colored, 5-beaded necklaces.

Allowing reflections cannot increase the number of equivalence classes, since any two necklaces that are related by a rotation remain related by that rotation when reflections are included.

Example 9.2.8: In accordance with the description of reflections in §9.1, each of the five reflections has the cycle structure $t_1 t_2^2$. It follows that the dihedral group \mathbb{D}_5 that includes all the reflections as well as the rotations has the cycle index

$$Z_{\mathbb{D}_5} = \frac{1}{10} (t_1^5 + 5t_1 t_2^2 + 4t_5)$$

Under dihedral symmetry the # of 2-colored, 5-beaded necklaces is

$$\frac{1}{10} (2^5 + 5 \cdot 2 \cdot 2^2 + 4 \cdot 2) = \frac{80}{10} = 8$$

In other words, for 2-colored, 4 beaded necklaces, dihedral symmetry yields no fewer equivalence classes of necklaces than cyclic symmetry.

However, allowing the reflections as well as the rotations might decrease the number of equivalence classes, since it is possible that two necklaces that are not equivalent under any rotation are equivalent under a reflection.

Example 9.2.9: Consider the 3-colored, 5-beaded necklaces. Under cyclic symmetry, the number of equivalence classes is

$$\frac{1}{5} (3^5 + 4 \cdot 3) = \frac{255}{5} = 51$$

By way of contrast, under dihedral symmetry, the number of classes is only

$$\frac{1}{10} (3^5 + 5 \cdot 3 \cdot 3^2 + 4 \cdot 3) = \frac{390}{10} = 39$$

Figure 9.2.6 illustrates two necklaces that are equivalent under a vertical reflection, and thus under dihedral symmetry. However, none of the five rotations on one necklace produces the other necklace, so they are not equivalent under cyclic symmetry.

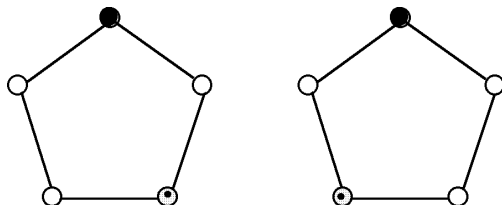


Fig 9.2.6 Two 3-colored necklaces that are equivalent under dihedral symmetry, but not under cyclic symmetry.

9.3 COUNT SMALL SIMPLE GRAPHS

Some best illustrations of Burnside-Pólya counting are in graph theory.

REVIEW FROM §0.6:

- A graph is a **simple graph** if every edge has two distinct endpoints and if no two edges have the same two endpoints. In a simple graph, an edge with endpoints u and v may be denoted uv .

DEF: An **automorphism of a simple graph** $G = (V, E)$ is a permutation $\pi : V \rightarrow V$ that preserves adjacency and non-adjacency. That is,

- if u and v are adjacent, then so are $\pi(u)$ and $\pi(v)$.
- if u and v are non-adjacent, then so are $\pi(u)$ and $\pi(v)$.

Vertex Automorphisms and Colorings

Prop 9.3.1. *The set of all automorphisms of a simple graph $G = (V, E)$ acts as a perm group on its vertex set.*

Proof: Composing two automorphisms preserves both adjacency and non-adjacency. Accordingly, the composition is an automorphism. \diamond

NOTATION: The automorphism group of the vertex set of a graph G is denoted $\text{Aut}_V(G)$.

Example 9.3.1: The graph W_5 in Figure 9.3.1 is called a *wheel graph* because it looks something like a wheel with five spokes.

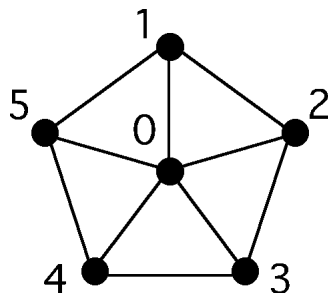


Fig 9.3.1 The wheel graph W_5 .

The automorphism group $\text{Aut}_V(W_5)$ has 5 rotations and 5 reflections, for a total of 10 perms. Its cycle index is

$$\mathcal{Z}_{\text{Aut}_V(W_5)}(t_1, \dots, t_6) = \frac{1}{10} (t_1^6 + 5t_1^2t_2^2 + 4t_1t_5)$$

The number of (≤ 2) -colorings is

$$\mathcal{Z}_{\text{Aut}_V(W_5)}(2, \dots, 2) = \frac{1}{10} (2^6 + 5 \cdot 2^2 \cdot 2^2 + 4 \cdot 2 \cdot 2) = 16$$

Table 9.3.1 calculates the Pólya inventory. Due to symmetry, the coefficients of

$$b^2w^4, \quad bw^5, \quad \text{and} \quad w^6$$

must be the same as the coefficients of

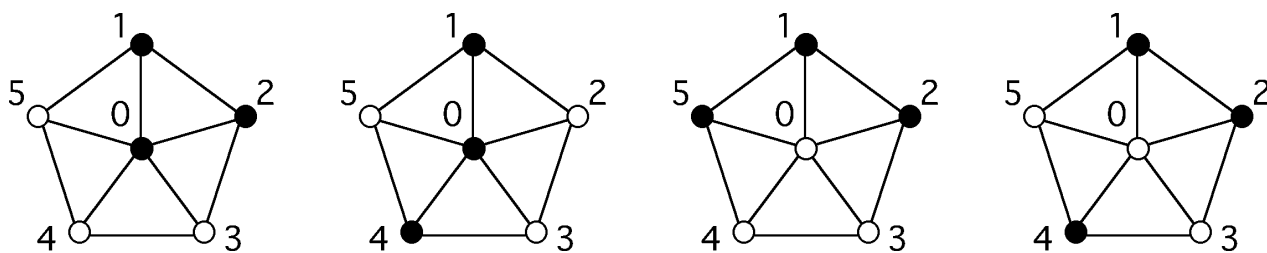
$$b^4w^2, \quad b^5w, \quad \text{and} \quad b^6$$

respectively. Thus, they may be omitted from the table.

Table 9.3.1 Pólya inv for (≤ 2) -colorings of $V(W_5)$.

$\zeta(\pi)$	subst	b^6	b^5w	b^4w^2	b^3w^3
t_1^6	$(b+w)^6$	1	6	15	20
$5t_1^2t_2^2$	$5(b+w)^2(b^2+w^2)^2$	5	10	15	20
$4t_1t_5$	$4(b+w)(b^5+w^5)$	4	4	0	0
sum		10	20	30	40
$\div 10$		1	2	3	4

Figure 9.3.2 illustrates the four colorings for the case of three black vertices and three white.

**Fig 9.3.2** Four (≤ 2) -colorings of the wheel graph W_5 .

Edge Automorphisms and Colorings

DEF: For any automorphism $\pi : V \rightarrow V$ of the vertex set of a simple graph $G = (V, E)$, there is an *induced edge automorphism* π_E given by the rule

$$\pi_E(uv) = \pi(u)\pi(v)$$

Example 9.3.1, cont.: The following translations of vertex automorphisms into edge automorphisms represent all three kinds of transformation of cycle structure.

$$\begin{aligned} (0)(1)(2)(3)(4)(5) &\mapsto (01)(02)(03)(04)(05)(12)(23)(34)(45)(50) \\ (0)(1\ 2\ 3\ 4\ 5) &\mapsto (01\ 02\ 03\ 04\ 05)(12\ 23\ 34\ 45\ 51) \\ (0)(1)(3\ 4)(2\ 5) &\mapsto (01)(34)(02\ 05)(03\ 04)(23\ 54)(12\ 15) \end{aligned}$$

Prop 9.3.2. *The set of all automorphisms of a simple graph $G = (V, E)$ acts as a perm group on its edge set.*

Proof: The composition of two edge automorphisms is an edge automorphism. \diamond

NOTATION: The automorphism group of the edge set of a graph G is denoted $\text{Aut}_E(G)$.

Example 9.3.1, cont.: The cycle index of $\text{Aut}_E(W_5)$ is

$$\mathcal{Z}_{\text{Aut}_E(W_5)}(t_1, \dots, t_{10}) = \frac{1}{10} (t_1^{10} + 5t_1^2 t_2^4 + 4t_5^2)$$

The number of (≤ 2) -colorings is

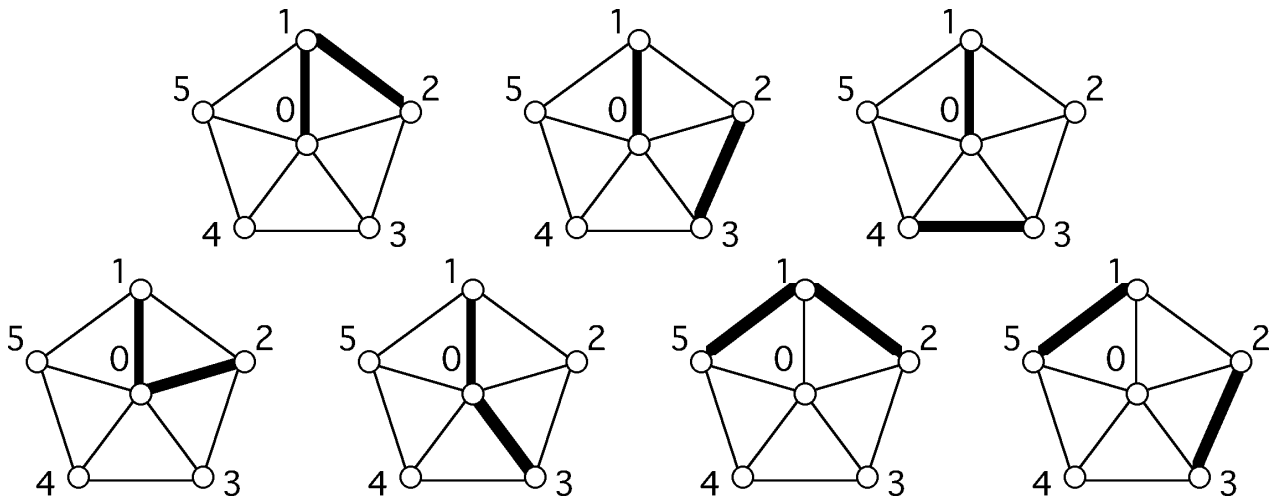
$$\mathcal{Z}_{\text{Aut}_E(W_5)}(2, \dots, 2) = \frac{1}{10} (2^{10} + 5 \cdot 2^2 \cdot 2^4 + 4 \cdot 2^2) = 136$$

Table 9.3.2 gives a partial inventory.

Table 9.3.2 Partial inv for (≤ 2) -colorings of $E(W_5)$.

$\zeta(\pi)$	subst	a^{10}	a^9b	a^8b^2	a^7b^3
t_1^{10}	$(a+b)^{10}$	1	10	45	120
$5t_1^2t_2^4$	$5(a+b)^2(a^2+b^2)^4$	5	10	25	40
$4t_5^2$	$4(a^5+b^5)^2$	4	0	0	0
sum		10	20	70	160
$\div 10$		1	2	7	16

Figure 9.3.3 shows the seven colorings for the case of eight light (a^8) edges and two dark (b^2) edges.

**Fig 9.3.3** Seven edge- a^8b^2 -colorings of the graph W_5 .

Orbits of Labeled Graphs

DEF: A *standard labeled graph* on n vertices is a simple graph whose vertices are identified with the numbers $1, 2, \dots, n$.

Proposition 9.3.3. *The number of standard labeled simple graphs on n vertices is*

$$2^{\binom{n}{2}}$$

Proof: Each possible edge ij is either absent or present.

◇

DEF: An *isomorphism of two simple graphs* G and H is a bijection $V_G \rightarrow V_H$ that preserves adjacency and non-adjacency of all pairs of vertices in V_G .

There are isomorphism relations among the standard labeled simple graphs.

Proposition 9.3.4. *The number of isomorphism types of n -vertex simple graphs equals the number of orbits of the action*

$$[\text{Aut}_E(K_n) : \text{Col}_2(E_{K_n})]$$

Proof: If the two colors used for coloring edges of K_n are regarded as *absent* and *present*, then the full set of 2^n edge- (≤ 2) -colorings is in one-to-one correspondence with the full set of n -vertex standard labeled simple graphs, and in this regard, the coloring classes correspond to the isomorphism types. ◇

Proposition 9.3.4 suggests the following general strategy for counting the isomorphism types of the n -vertex simple graphs. It is illustrated by a series of propositions for counting the isomorphism types of simple graphs with 4 and 5 vertices.

Step 1: Calculate cycle-index polynomial of $\text{Aut}_V(K_n)$.

Since knowing the cycle-index polynomial is sufficient for algebraic counting, writing out all the permutations in a large permutation group can be avoided.

Step 2: Calculate cycle-index polynomial of $\text{Aut}_E(K_n)$.

The cycle-index polynomial of $\text{Aut}_E(K_n)$ is obtained by considering each cycle size and each pair of cycle sizes in the cycle-index polynomial of $\text{Aut}_V(K_n)$.

Step 3: Apply Theorem 9.4.8.

This final step in counting the isomorphism types of graphs with n vertices is to simply substitute the number 2 for every variable in the cycle-index polynomial $Z_{\text{Aut}_E(K_n)}$.

Simple Graphs on 4 Vertices

The following three propositions implement the general counting strategy for the 4-vertex simple graphs.

Prop 9.3.5. *The permutation action $[\text{Aut}_V(K_4) : V_{K_4}]$ has the following cycle-index polynomial.*

$$Z_{\text{Aut}_V(K_4)}(t_1, t_2, t_3, t_4) = \frac{1}{24}(t_1^4 + 6t_1^2t_2 + 8t_1t_3 + 3t_2^2 + 6t_4)$$

Proof: The 24 vertex-perms in $\text{Aut}_V(K_4)$ are naturally partitioned according to the five possible cycle structures:

$$t_1^4 \quad t_1^2t_2 \quad t_1t_3 \quad t_2^2 \quad t_4$$

Each cell in this partition is to be counted.

t_1^4 : 1 automorphism.

Only the identity perm has this cycle structure.

$t_1^2 t_2$: 6 automorphisms.

The number of ways to choose two vertices for the 2-cycle is

$$\binom{4}{2} = 6$$

$t_1 t_3$: 8 automorphisms.

The number of ways to choose three vertices for the 3-cycle is

$$\binom{4}{3} = 4$$

and the number of ways to arrange them in a cycle is $(3 - 1)! = 2$.

t_2^2 : 3 automorphisms.

There are three ways to group four objects into two cycles, when it does not matter which cycle is written first.

t_4 : 6 automorphisms.

They correspond to the $(4 - 1)! = 6$ ways that four objects can be arranged in a cycle. \diamond

Prop 9.3.6. *The permutation action $[\text{Aut}_E(K_4) : E_{K_4}]$ has the following cycle-index polynomial.*

$$\mathcal{Z}_{\text{Aut}_E(K_4)}(t_1, t_2, t_3, t_4) = \frac{1}{24}(t_1^6 + 9t_1^2 t_2^2 + 8t_3^2 + 6t_2 t_4)$$

Proof: The size of the cycle to which an edge belongs is determined by the cycles to which its endpoints belong. Thus, for every automorphism $\pi \in \text{Aut}_E(K_n)$, the cycle structure $\zeta(\pi_E)$ of the edge-permutation is determined by the the cycle structure $\zeta(\pi_V)$ of the vertex-permutation.

Case 1. If $\zeta(\pi_V) = t_1^4$, then $\zeta(\pi_E) = t_1^6$.

Justification: If both endpoints of a given edge e are in a 1-cycle of the vertex-permutation π_V , then they are both fixed points. In a simple graph, the corresponding edge-permutation must map that edge to itself.

Case 2. If $\zeta(\pi_V) = t_1^2 t_2$, then $\zeta(\pi_E) = t_1^2 t_2^2$.

Justification: An edge of K_4 is mapped to itself if both its endpoints are in a 2-cycle or if each endpoint is in a 1-cycle. Thus, two edges of K_4 are fixed by π_V . Each of the other four edges has one endpoint in a 1-cycle, which is fixed by π_V , and the other in a 2-cycle of π_V , which is mapped by π_V to the other vertex in that 2-cycle. It follows that such an edge lies in a 2-cycle of π_E .

Case 3. If $\zeta(\pi_V) = t_1 t_3$, then $\zeta(\pi_E) = t_3^2$.

Justification: The three edges of K_4 that have both their ends in the 3-cycle of π_V lie in a 3-cycle of π_E . The three edges of K_4 that have one endpoint in a 1-cycle of π_V and the other endpoint in a 3-cycle all lie in another 3-cycle of π_E .

Case 4. If $\zeta(\pi_V) = t_2^2$, then $\zeta(\pi_E) = t_1^2 t_2^2$.

Justification: The two edges that have both endpoints in the same 2-cycle of π_V are both fixed by π_E . If an edge has one endpoint in one 2-cycle of π_V and the other endpoint in another 2-cycle of π_V , then that edge lies in a 2-cycle of π_E with the edge whose respective endpoints are the other vertices of those 2-cycles of π_V .

Case 5. If $\zeta(\pi_V) = t_4$, then $\zeta(\pi_E) = t_2t_4$.

Justification: The four edges whose endpoints are consecutive vertices in the 4-cycle of π_V form a cycle of π_E . The two edges whose endpoints are spaced 2 apart in the 4-cycle of π_V form a 2-cycle of π_E . \diamond

Cor 9.3.7. *There are exactly 11 isomorphism types of simple graph with 4 vertices. (The 11 graphs promised by this calculation are shown in Figure 9.3.4.)*

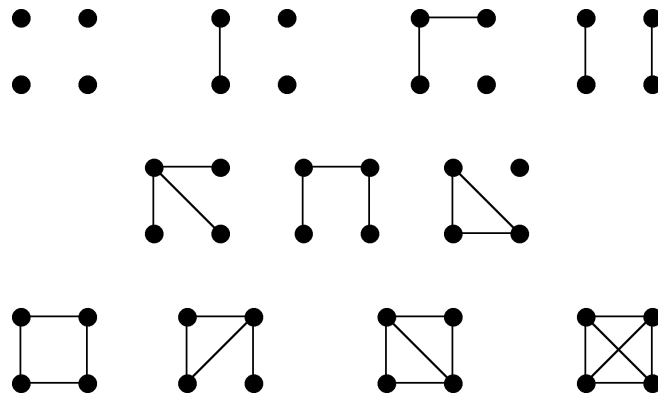


Fig 9.3.4 The 11 simple 4-vertex graphs.

Proof: Prop 9.3.6 asserts that $\mathcal{Z}_{\text{Aut}_E(K_4)}(2, 2, 2, 2)$

$$= \frac{1}{24} (2^6 + 9 \cdot 2^2 \cdot 2^2 + 8 \cdot 2^2 + 6 \cdot 2 \cdot 2) = 11 \quad \diamond$$

Observe that the Pólya inventory in Table 9.3.3 is consistent with Figure 9.3.4. The indeterminates a and p stand for *absent* and *present*. They are Pólya-substituted into the cycle index to produce the table.

$$\mathcal{Z}_{\text{Aut}_E(K_4)}(t_1, t_2, t_3, t_4) = \frac{1}{24}(t_1^6 + 9t_1^2t_2^2 + 8t_3^2 + 6t_2t_4)$$

For instance, the coefficient of 2 for the monomial a^4p^2 at the bottom of the column labeled a^4p^2 signifies that there are exactly two 4-vertex graphs with exactly 2 edges present.

Table 9.3.3 Isomorphism types of 4-vertex graph.

$\zeta(\pi_E)$	subst	a^6	a^5p	a^4p^2	a^3p^3
t_1^6	$(a + p)^6$	1	6	15	20
$9t_1^2t_2^2$	$9(a + p)^2(a^2 + p^2)^2$	9	18	27	36
$8t_3^2$	$8(a^3 + p^3)^2$	8	0	0	16
$6t_2t_4$	$6(a^2 + p^2)(a^4 + p^4)$	6	0	6	0
sum		24	24	48	72
$\div 24$		1	1	2	3

Simple Graphs with 5 Vertices

Proposition 9.3.8. *There are exactly 34 isomorphism types of simple graph with 5 vertices.*

Proof: By using the same approach as in the calculation of the number of 4-vertex simple graphs, it can be shown (an explicit general method for any number of vertices is given in the next section) that $\mathcal{Z}_{\text{Aut}_V(K_5)}(t_1, \dots, t_5)$

$$= \frac{1}{120} (t_1^5 + 10t_1^3t_2 + 15t_1t_2^2 + 20t_1^2t_3 + 20t_2t_3 + 30t_1t_4 + 24t_5)$$

Therefore, $\mathcal{Z}_{\text{Aut}_E(K_5)}(t_1, \dots, t_{10})$

$$= \frac{1}{120} (t_1^{10} + 10t_1^4t_2^3 + 15t_1^2t_2^4 + 20t_1t_3^3 + 20t_1t_3t_6 + 30t_2t_4^2 + 24t_5^2)$$

and accordingly $\mathcal{Z}_{\text{Aut}_E(K_5)}(2, \dots, 2)$

$$= \frac{1}{120} (2^{10} + 10 \cdot 2^7 + 15 \cdot 2^6 + 20 \cdot 2^4 + 20 \cdot 2^3 + 30 \cdot 2^3 + 24 \cdot 2^2) = 34 \quad \diamond$$

Partial Pólya Inventories

Doing a hand calculation of a complete Pólya inventory can be quite tedious. We complete this section by considering how to calculate the number of 5-vertex graphs with 4 edges, to illustrate how to do a selective partial inventory. Table 9.3.4 summarizes the calculation.

Table 9.3.4 Counting 5-vertex graphs with 3 edges.

$\zeta(\pi_E)$	substitute	a^7p^3 – contribution	eval
t_1^{10}	$(a+p)^{10}$	$1 \cdot \binom{10}{3}$	120
$10t_1^4t_2^3$	$10(a+p)^4(a^2+p^2)^3$	$10 \cdot \left[\binom{4}{1} \binom{3}{1} + \binom{4}{3} \binom{3}{0} \right]$	160
$15t_1^2t_2^4$	$15(a+p)^2(a^2+p^2)^4$	$15 \cdot \binom{2}{1} \binom{4}{1}$	120
$20t_1t_3^3$	$20(a+p)(a^3+p^3)^3$	$20 \cdot \binom{1}{0} \binom{3}{1}$	60
$20t_1t_3t_6$	$20(a+p)(a^3+p^3)(a^6+p^6)$	$20 \binom{1}{0} \binom{1}{1} \binom{1}{0}$	20
$30t_2t_4^2$	$30(a^2+p^2)(a^4+p^4)^2$	0	
$24t_5^2$	$24(a^5+p^5)^2$	0	
sum			480
	$\div 120$		$= 4$

Example 9.3.2: When the expression

$$10(a+p)^4(a^2+p^2)^3$$

on the second line of the table is fully expanded, there are two contributions to the term with the monomial a^7p^3 . One results from the product

$$12a^7p^3 \text{ of the terms } 4a^3p^1 \text{ and } 3a^4p^2$$

in the expansions of $(a+p)^4$ and $(a^2+p^2)^3$, respectively, and the other results from the product

$$4a^7p^3 \text{ of the terms } 4a^1p^3 \text{ and } 1a^6p^0$$

in the expansions of $(a+p)^4$ and $(a^2+p^2)^3$, respectively. The sum $12+4$ is multiplied by the coefficient 10 to yield 160.

9.4 PARTITIONS OF INTEGERS

In the cycle index $\mathcal{Z}_{\text{Aut}_V(K_n)}(t_1, \dots, t_n)$, each term is the product of a cycle structure

$$t_1^{e_1} t_2^{e_2} \cdots t_n^{e_n}$$

and a coefficient giving the number of permutations in the group $\text{Aut}_V(K_n)$ having that cycle structure. The sum of the coefficients is $n!$, since there are $n!$ permutations in all.

Example 9.4.1: In the previous section, we calculated (see (9.4.1)) that

$$\mathcal{Z}_{\text{Aut}_V(K_4)}(t_1, t_2, t_3, t_4) = \frac{1}{24}(t_1^4 + 6t_1^2 t_2 + 8t_1 t_3 + 3t_2^2 + 6t_4)$$

and (see (9.4.2)) that

$$\begin{aligned} \mathcal{Z}_{\text{Aut}_V(K_5)}(t_1, \dots, t_5) = \\ \frac{1}{120}(t_1^5 + 10t_1^3 t_2 + 15t_1 t_2^2 + 20t_1^2 t_3 + 20t_2 t_3 + 30t_1 t_4 + 24t_5) \end{aligned}$$

DEF: A *partition of an integer* n (with n positive) is a sum

$$s_1 + s_2 + \cdots + s_k$$

whose value is n and whose summands are positive integers. It is usually represented with the summands in nonincreasing order, without the addition signs.

The cycle structure $t_1^{e_1} t_2^{e_2} \cdots t_n^{e_n}$ of a permutation corresponds to the integer partition

$$\underbrace{\overbrace{n \ n \ \cdots \ n}^{e_n \ n's}} \cdots \underbrace{\overbrace{2 \ 2 \ \cdots \ 2}^{e_2 \ 2's}} \underbrace{\overbrace{1 \ 1 \ \cdots \ 1}^{e_1 \ 1's}}$$

Example 9.4.1, cont.: The five partitions of 4 are

$$1111 \quad 211 \quad 22 \quad 31 \quad 4$$

Observe that they correspond to the terms of the cycle index polynomial

$$\mathcal{Z}_{\text{Aut}_V(K_4)}(t_1, t_2, t_3, t_4) = \frac{1}{24}(t_1^4 + 6t_1^2 t_2 + 8t_1 t_3 + 3t_2^2 + 6t_4)$$

Similarly, the seven partitions of the integer 5

$$11111 \quad 2111 \quad 221 \quad 311 \quad 32 \quad 41 \quad 5$$

correspond to the terms of the cycle index polynomial

$$\begin{aligned} \mathcal{Z}_{\text{Aut}_V(K_5)}(t_1, \dots, t_5) = \\ \frac{1}{120}(t_1^5 + 10t_1^3 t_2 + 15t_1 t_2^2 + 20t_1^2 t_3 + 20t_2 t_3 + 30t_1 t_4 + 24t_5) \end{aligned}$$

Listing all Partitions of an Integer

As an aid in calculating the cycle index polynomial $\mathcal{Z}_{\text{Aut}_V(K_n)}(t_1, \dots, t_n)$ for the automorphism group of a complete graph of general size, we now introduce a systematic way to list all partitions of an arbitrary integer n .

In Example 9.4.1, the partitions of 5 are given in ascending order. Algo 9.4.1 lists all the partitions of n in descending order. The key step of constructing the next partition after $s_1 s_2 \cdots s_k$ has a relatively easy intuitive description. It is assumed that the parts s_i of the partition given as input are written in order of descending size.

Algorithm 9.4.1: Next Integer Partition (S)

Input: an integer partition $S = s_1 \cdots s_k$, not all 1's.

Output: The next integer partition, in descending order.

Assign $b := \max\{j \mid s_j \neq 1\}$.

Assign $M := s_b - 1$.

Assign $s_b := M$.

Replace suffix $s_{b+1} \cdots s_k$ **by** string of $\lfloor k - j + 1/M \rfloor$ M 's.

If $k - j + 1 \bmod M > 0$

then append integer $k - j + 1 \bmod M$ to string S .

Return (S)

Example 9.4.2: We apply Algo 9.4.1 to the partition

8666411111

of the integer 35. Then index b is 5, the location of the rightmost non-1, whose value s_5 is 4, so $M = 3$. The assignment $s_5 := M$ decreases the value of s_5 to 3. The suffix of five 1's is replaced by two 3's, since $\lfloor 6/3 \rfloor = 2$. The division has zero remainder. Thus, the partition returned is

8666333

To obtain a list all the partitions of an integer n , that integer itself is supplied to the algorithm Next Integer Partition to initiate the list. Then the output is supplied to the algorithm iteratively, until a string of n 1's is obtained as the final partition.

Example 9.4.3: For $n = 6$, iterative application of Next Integer Partition produces the sequence

$$6 \rightarrow 51 \rightarrow 42 \rightarrow 411 \rightarrow 33 \rightarrow 321 \rightarrow 3111 \\ \rightarrow 222 \rightarrow 2211 \rightarrow 21111 \rightarrow 111111$$

Ferrers Diagrams

DEF: The *Ferrers diagram* of a partition $s_1 s_2 \cdots s_k$ is an array of k rows of dots, with s_j dots in row j .

Example 9.4.4: The partition 6441 has the Ferrers diagram

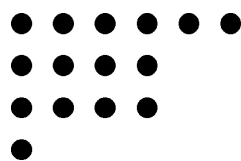


Fig 9.4.1 Ferrers diagram for the integer partition 6441.

DEF: The *conjugate of a Ferrers diagram* for the partition $s_1 s_2 \cdots s_k$ is the Ferrers diagram with k columns of dots, with s_j dots in column j .

Example 9.4.4, cont.: The conjugate of the Ferrers diagram in Figure 9.4.1 is the diagram

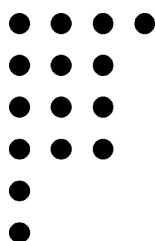


Fig 9.4.2 Conjugate of the previous Ferrers diagram.

DEF: The *conjugate of a partition* S is the partition whose Ferrers diagram is the conjugate of the Ferrers diagram of S .

Ferrers diagrams are the easiest way to prove the following kind of theorem about partitions.

Thm 9.4.1. *The number of partitions of an integer n into at most k parts equals the number of partitions of n into parts of size at most k .*

Proof: The conjugation operation on Ferrers diagrams is bijective from the set of partitions of n into at most k parts, to the set of partitions of n of size at most k . \diamond

Partition Lattices

DEF: The *inclusion relation on integer partitions* is given by

$$s_1 s_2 \cdots s_k \preceq u_1 u_2 \cdots u_\ell \quad \text{if } k \leq \ell$$

$$\text{and } s_j \leq u_j, \quad \text{for } j = 1, \dots, k$$

Its name reflects the fact that the Ferrers diagram of the first is contained in the Ferrers diagram of the second.

DEF: For an integer partition $S = s_1 s_2 \cdots s_k$, the *Young's lattice* \mathcal{Y}_S has as its domain the set of all integer partitions included in S . The partial ordering is inclusion.

Example 9.4.5: The Hasse diagram for the Young's lattice for the integer partition 3221 is shown in Figure 9.4.3.

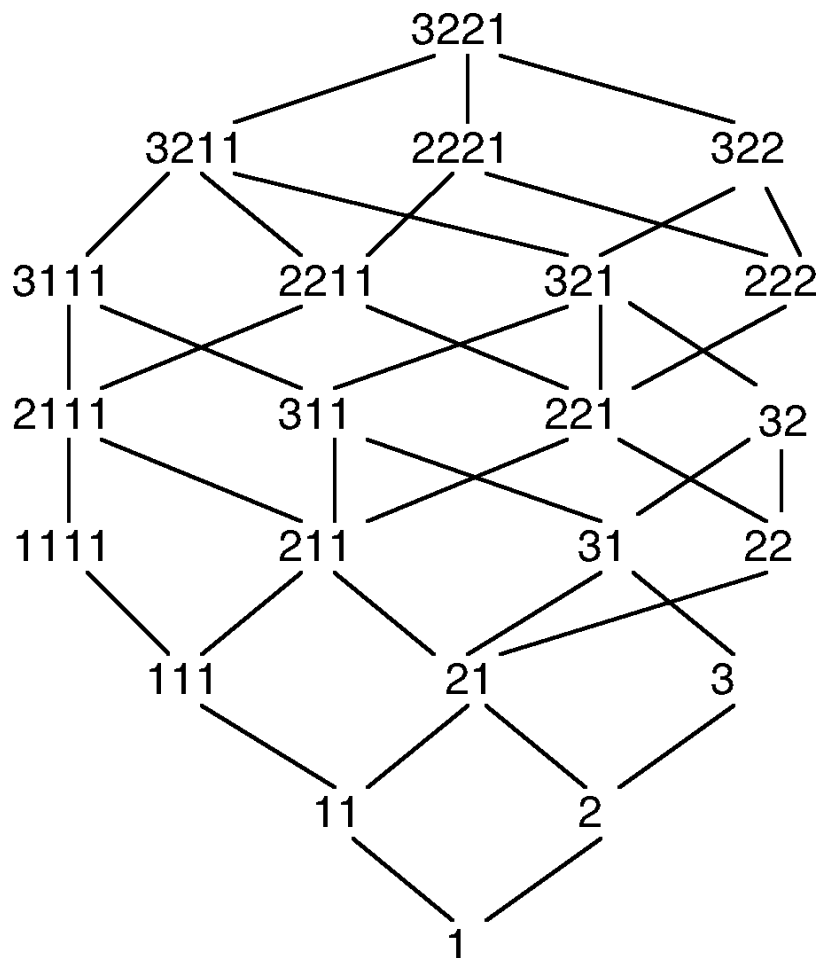


Fig 9.4.3 Young's lattice \mathcal{Y}_{3221} .

A Young's lattice is graded. The rank of each partition is the integer it partitions. There is a second kind of lattice for partitions of integers, in which all the elements partition the same integer.

DEF: Let $B = b_1 b_2 \cdots b_k$ and $U = u_1 u_2 \cdots u_\ell$ be any two partitions of the integer n , such that

$$b_1 + \cdots + b_j \leq u_1 + \cdots + u_j \quad \text{for all } j \leq \min(k, \ell)$$

Then the partition U has **summation dominance** over the partition B . The resulting poset \mathcal{SD}_n is called a **summation dominance lattice**.

Proposition 9.4.2. *The order of the partitions of an integer n produced by iterative application of the algorithm *Next Integer Partition* is a linear extension of the summation dominance partial ordering.*

Proof: Since the input to the algo has lexicographic dominance over the output, it cannot be summation dominated by the output. \diamond

Example 9.4.6: A Hasse diagram for the summation dominance lattice \mathcal{D}_7 is shown in Figure 9.4.4. Observe that it is unranked.

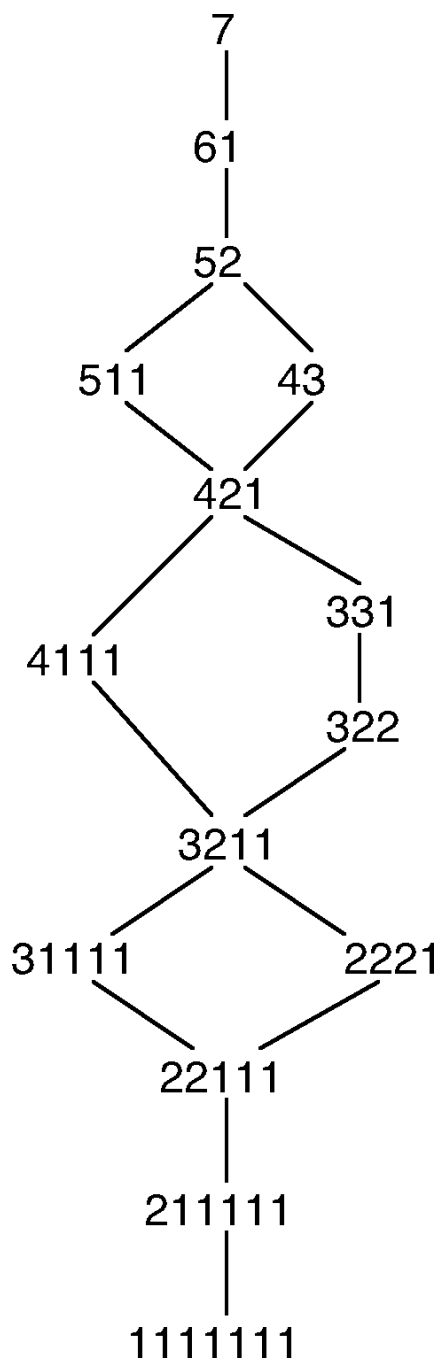


Fig 9.4.4 Summation dominance lattice SD_7 .

9.5 CALCULATING A CYCLE INDEX

Beyond writing a cycle structure monomial $t_1^{e_1} \cdots t_n^{e_n}$ corresponding to each partition of an integer n , calculating the cycle index of $\text{Aut}_V(K_n)$ requires writing the coeff of each such monomial. When calculating $\text{Aut}_E(K_n)$, another step is transforming a cycle structure for the automorphism action on the vertices of the complete graph K_n to the corresponding cycle structure for the automorphism action on the edges of K_n .

Multinomial Coefficients

DEF: Let r_1, r_2, \dots, r_k be a list of non-negative integers whose sum is n . The value of the ***multinomial coeff***

$$\binom{n}{r_1 \quad r_2 \quad \cdots \quad r_k}$$

is the number of ways that a set of n distinct objects can be distributed into k distinct boxes

$$B_1, B_2, \dots, B_k$$

so that, for $j = 1, \dots, k$, there are r_j objects in box B_j . The multinomial coeff generalizes the binomial coeff

$$\binom{n}{r}$$

which is the special case with two boxes, the first of size r , and the second of size $n - r$.

Proposition 9.5.1. *Let r_1, r_2, \dots, r_k be a list of non-negative integers whose sum is n . Then*

$$\binom{n}{r_1 \ r_2 \ \cdots \ r_k} = \frac{n!}{r_1! r_2! \cdots r_k!}$$

Proof: For $k = 2$, the right side is a familiar formula for the value of the binomial coeff. We continue inductively.

Clearly, the number of ways to distribute n objects into the boxes

$$B_1, B_2, \dots, B_k$$

of sizes r_1, r_2, \dots, r_k equals the product of the number of ways to select r_1 objects for box B_1 and the number of ways to distribute the remaining $n - r_1$ objects into the boxes B_2, B_3, \dots, B_k . That is,

$$\binom{n}{r_1 \ r_2 \ \cdots \ r_k} = \binom{n}{r_1} \binom{n - r_1}{r_2 \ r_3 \ \cdots \ r_k} \quad (9.5.1)$$

By the induction hypothesis,

$$\binom{n - r_1}{r_2 \ r_3 \ \cdots \ r_k} = \frac{(n - r_1)!}{r_2! r_3! \cdots r_k!} \quad (9.5.2)$$

Thus, combining Equations (9.5.1) and (9.5.2),

$$\begin{aligned} \binom{n}{r_1 \ r_2 \ \cdots \ r_k} &= \binom{n}{r_1} \frac{(n - r_1)!}{r_2! r_3! \cdots r_k!} \\ &= \frac{n!}{r_1! r_2! \cdots r_k!} \quad \diamond \end{aligned}$$

Example 9.5.1, cont.: It follows from Proposition 9.5.1 that the number of ways to partition an executive board into three committees of 2, 3, and 3 is

$$\frac{8!}{2!3!3!} = 560$$

Non-distinct Boxes

When a perm π partitions n objects into disjoint cycles, the cycles are non-distinct. For instance, the perms

$$(1\ 2)(3\ 7\ 5)(4\ 6\ 8) \quad \text{and} \quad (1\ 2)(4\ 6\ 8)(3\ 7\ 5)$$

are identical, since the order in which the 3-cycles are written in a disjoint cycle representation has no bearing on the effect of the permutation.

Proposition 9.5.2. *Let r_1, r_2, \dots, r_k and e_1, e_2, \dots, e_k be list of non-negative integers such that*

$$n = e_1 r_1 + e_2 r_2 + \dots + e_k r_k$$

Then the # ways to partition n distinct objects into non-distinct boxes, with e_j boxes of size r_j , for $j = 1, \dots, k$, is

$$\frac{n!}{(r_1!)^{e_1} (r_2!)^{e_2} \dots (r_k!)^{e_k} e_1! e_2! \dots e_k!}$$

Proof: If the boxes were distinct, the number of possible distributions would be

$$\frac{n!}{(r_1!)^{e_1} (r_2!)^{e_2} \dots (r_k!)^{e_k}}$$

by Proposition 9.5.1. Application of the Rule of Quotient motivates division by

$$e_1!e_2!\cdots e_k!$$

for non-distinct boxes. ◇

Example 9.5.2: The three ways to partition the integer six into three parts are 411, 321, and 222. The Stirling subset number

$$\left\{ \begin{matrix} 6 \\ 3 \end{matrix} \right\}$$

is the total number of ways to partition 6 objects into 3 cells. Thus, in view of Proposition 9.5.2, we anticipate the result of the following computation.

$$\begin{aligned} \left\{ \begin{matrix} 6 \\ 3 \end{matrix} \right\} &= \binom{6}{4 \ 1 \ 1} \frac{1}{2!} + \binom{6}{3 \ 2 \ 1} + \binom{6}{2 \ 2 \ 2} \frac{1}{3!} \\ &= \frac{6!}{4!} \cdot \frac{1}{2!} + \frac{6!}{3!2!} + \frac{6}{2!2!2!} \cdot \frac{1}{3!} \\ &= 15 + 60 + 15 \\ &= 90 \end{aligned}$$

Corollary 9.5.3. *The number of permutations of cycle structure $t_1^{e_1} \cdots t_n^{e_n}$ in $\text{Aut}_V(K_n)$ is*

$$\binom{n}{\underbrace{e_1 r'_1 s}_{r_1 \cdots r_1} \quad \cdots \quad \underbrace{e_k r'_k s}_{r_k \cdots r_k}} \frac{((r_1 - 1)!)^{e_1} \cdots ((r_k - 1)!)^{e_k}}{e_1! \cdots e_k!}$$

Proof: Proposition 9.5.2 accounts for the multinomial coefficient and for the denominator of the fraction. The numerator of the fraction accounts for the objects within each cell into a cycle of the permutation. The number of ways to organize s objects into a cycle is $(s - 1)!$. \diamond

Example 9.5.2, cont.: The Stirling cycle number $\left[\begin{smallmatrix} 6 \\ 3 \end{smallmatrix} \right]$ is the number of permutations of 6 objects with three cycles. Thus, consistent with Corollary 9.5.3, we obtain

$$\begin{aligned} \left[\begin{smallmatrix} 6 \\ 3 \end{smallmatrix} \right] &= \binom{6}{4 \ 1 \ 1} \frac{3!0!0!}{1!2!} + \binom{6}{3 \ 2 \ 1} \frac{2!1!0!}{1!1!1!} + \binom{6}{2 \ 2 \ 2} \frac{1!1!1!}{3!} \\ &= \frac{6!}{4!} \cdot 3 + \frac{6!}{3!2!} \cdot 2 + \frac{6!}{2!2!2!} \cdot \frac{1}{6} \\ &= 90 + 120 + 15 \\ &= 225 \end{aligned}$$

Prop 9.5.4. *The cycle index of the group $\text{Aut}_V(K_6)$ is*

$$\begin{aligned} Z_{\text{Aut}_V(K_6)}(t_1, \dots, t_6) &= \frac{1}{720} (t_1^6 + 15t_1^4t_2 + 45t_1^2t_2^2 + 15t_2^3 + 40t_1^3t_3 \\ &\quad + 120t_1t_2t_3 + 40t_3^2 + 90t_1^2t_4 + 90t_2t_4 + 144t_1t_5 + 120t_6) \end{aligned}$$

Proof: This follows from Corollary 9.5.3. \diamond

Transforming the Cycle Index

When counting isomorphism types of graphs, one further step is to transform each vertex automorphism cycle structure into the corresponding edge automorphism cycle structure. This step may vary, according to the kind of graphs being counted. What follows here is for counting simple graphs.

We continue to use variables t_j in the cycle structure of a graph automorphism action on the set of vertices. For clarity, we will use variables y_j in the cycle structure of the corresponding action on the set of edges.

Thm 9.5.5. *Let π be an automorphism of K_n , represented by perms π_V on V_{K_n} and π_E on E_{K_n} . Then*

$$(i) \ t_{2p+1} \rightarrow y_{2p+1}^p:$$

Each $(2p + 1)$ -cycle in π_V corresponds to p $(2p + 1)$ -cycles in π_E .

$$(ii) \ t_{2p} \rightarrow y_{2p}^{p-1} y_p:$$

Each $(2p)$ -cycle in π_V corresponds to $p - 1$ $(2p)$ -cycles and one p -cycle in π_E .

$$(iii) \ t_p t_q \rightarrow y_{\text{lcm}(p,q)}^{\text{gcd}(p,q)}:$$

Each $(p$ -cycle, q -cycle)-pair in perm π_V , with $p \neq q$, corresponds to $\text{gcd}(p, q)$ $\text{lcm}(p, q)$ -cycles in π_E .

$$(iv) \ t_p t_p \rightarrow y_p^p:$$

Each pair of p -cycles in π_V corresponds to p p -cycles in π_E .

Proof: The key to all four parts of the proof is that if ij is any edge in K_n , then the endpoints of the edge $\pi_E(ij)$ are $\pi_V(i)$ and $\pi_V(j)$. We begin each part with an illustrative example.

(i) $t_{2p+1} \rightarrow y_{2p+1}^p$:

The case $p = 2$, where we consider a factor t_5 corresponding to some 5-cycle $(1\ 2\ 3\ 4\ 5)$ in π_V , is illustrated in Figure 9.5.1. The copy of K_5 in Figure 9.5.1 is the induced subgraph of K_n on the five vertices 1, 2, 3, 4, and 5. Since π_E maps the edge 12 to the edge 23, maps 23 to 34, and so on, it must contain the cycle $(12\ 23\ 34\ 45\ 15)$, whose edges are solid lines in the figure.

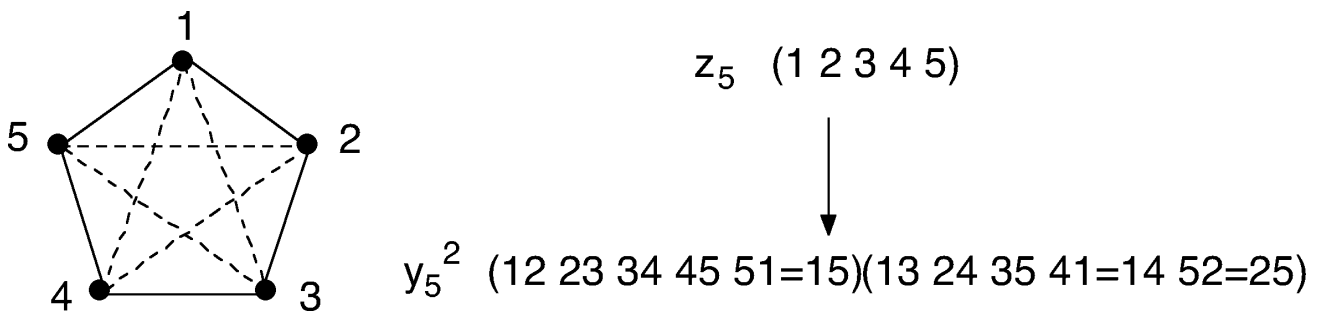


Fig 9.5.1 Transformation of t_5 into y_5^2 .

Since π_E maps the edge 13 to the edge 24, maps 24 to 35, and so on, it must also contain the cycle $(13\ 24\ 35\ 41\ 52)$, whose edges are dashed lines in the figure.

More generally, for a cycle in π_V of the form

$$(v_1 \quad v_2 \quad \cdots \quad v_{2p+1})$$

the $p - 1$ corresponding $(2p + 1)$ -cycles in π_E are

$$\begin{pmatrix} v_1 v_2 & v_2 v_3 & \cdots & v_{2p+1} v_1 \\ v_1 v_3 & v_2 v_4 & \cdots & v_{2p+1} v_2 \\ & & \vdots & \\ v_1 v_p & v_2 v_{p+1} & \cdots & v_{2p+1} v_{p-1} \\ v_1 v_{p+1} & v_2 v_{p+2} & \cdots & v_{2p+1} v_p \end{pmatrix}$$

(ii) $t_{2p} \rightarrow y_{2p}^{p-1} y_p$:

For the case $p = 3$, we consider a factor t_6 corresponding to a 6-cycle $(1\ 2\ 3\ 4\ 5\ 6)$ in π_V , as illustrated in Figure 9.5.2. The dark solid edges form one 6-cycle in π_E . Even though the dashed edges form two 3-cycles in the copy of K_6 in the figure, they all lie in the same 6-cycle of π_E . Even though the three light solid edges form no cycles in K_6 , they form a 3-cycle in π_E .

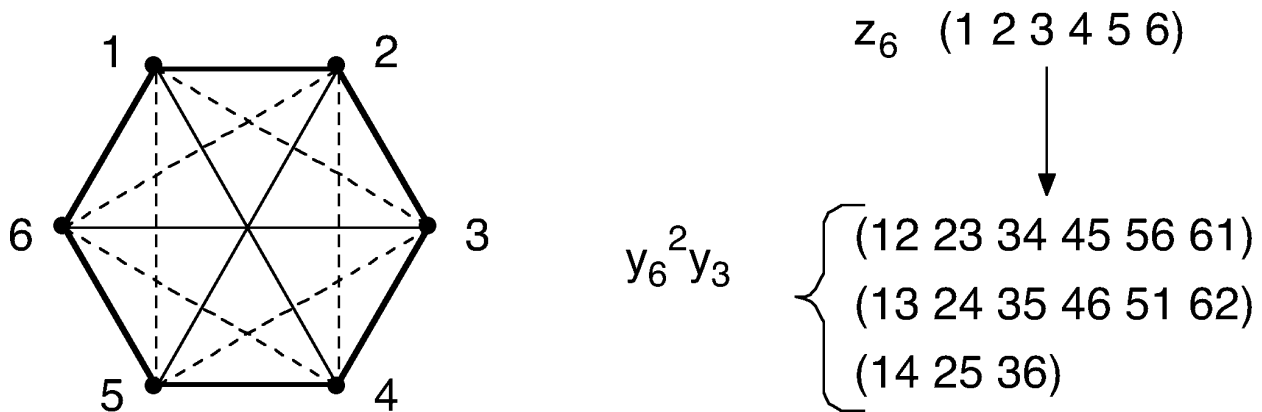


Fig 9.5.2 Transformation of t_6 into $y_6^2 y_3$.

In general, for a cycle in π_V of the form

$$(v_1\ v_2\ \cdots\ v_{2p})$$

the corresponding cycles in π_E are

$$\left. \begin{array}{l} (v_1 v_2 \quad v_2 v_3 \quad \cdots \quad v_{2p} v_1) \\ (v_1 v_3 \quad v_2 v_4 \quad \cdots \quad v_{2p} v_2) \\ \vdots \\ (v_1 v_p \quad v_2 v_{p+1} \quad \cdots \quad v_{2p} v_{p-1}) \\ (v_1 v_{p+1} \quad v_2 v_{p+2} \quad \cdots \quad v_p v_{2p}) \end{array} \right\} \begin{array}{l} p-1 \text{ } (2p)\text{-cycles} \\ \text{one } p\text{-cycle} \end{array}$$

(iii) $t_p t_q \rightarrow y_{\text{lcm}(p,q)}^{\text{gcd}(p,q)}$:

We consider two cycles $(1 \cdots 4)$ and $(\underline{1} \cdots \underline{6})$ in π_V , which yields $\text{gcd}(4,6) = 2$ cycles in π_E , each of length $\text{lcm}(4,6) = 12$. For clarity in Figure 9.5.3, these two cycles in π_E are shown separately. Neither is a cycle in the graph, only in the permutation.

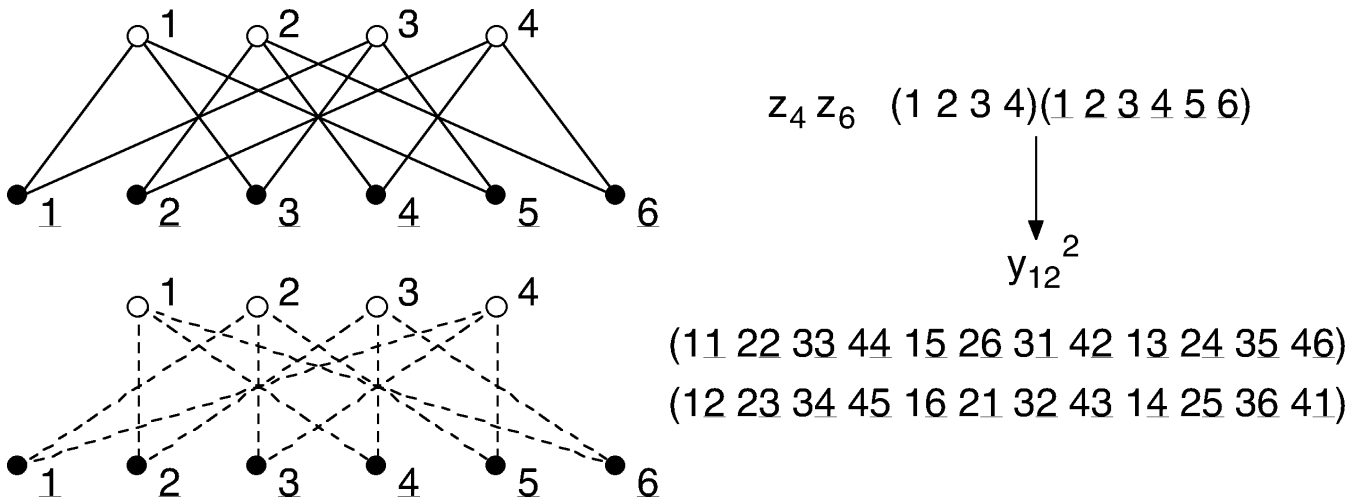


Fig 9.5.3 Transformation of $t_4 t_6$ into y_{12}^2 .

In general, for a pair of cycles in π_V

$$(u_1 \quad u_2 \quad \cdots \quad v_p) \quad \text{and} \quad (v_1 \quad v_2 \quad \cdots \quad v_q)$$

the $\gcd(p, q)$ corresponding $\text{lcm}(p, q)$ -cycles in π_E are

$$\begin{pmatrix} u_1 v_1 & u_2 v_2 & \cdots & u_p v_q \\ u_1 v_2 & u_2 v_3 & \cdots & u_p v_1 \\ \vdots & & & \\ u_1 v_{\gcd(p,q)} & u_2 v_{\gcd(p,q)+1} & \cdots & u_p v_{\gcd(p,q)-1} \end{pmatrix}$$

In the special case of two p -cycles in π_V , there are p p -cycles in π_E .

This completes the proof of the theorem. \diamond

Proposition 9.5.6. *There are exactly 156 isomorphism types of simple graph with 6 vertices.*

Proof: By Proposition 9.5.4, $\mathcal{Z}_{\text{Aut}_V(K_6)}(t_1, \dots, t_6)$

$$\begin{aligned} &= \frac{1}{720} (t_1^6 + 15t_1^4 t_2 + 45t_1^2 t_2^2 + 15t_2^3 + 40t_1^3 t_3 + 120t_1 t_2 t_3 \\ &\quad + 40t_3^2 + 90t_1^2 t_4 + 90t_2 t_4 + 144t_1 t_5 + 120t_6) \end{aligned}$$

By Theorem 9.5.5, $\mathcal{Z}_{\text{Aut}_E(K_6)}(y_1, \dots, y_{15})$

$$\begin{aligned} &= \frac{1}{720} (y_1^{15} + 15y_1^7 y_2^4 + 45y_1^3 y_2^6 + 15y_1^3 y_2^6 + 40y_1^3 y_3^4 + 120y_1 y_2 y_3^2 y_6 \\ &\quad + 40y_3^5 + 90y_1 y_2 y_4^3 + 90y_1 y_2 y_4^3 + 144y_5^3 + 120y_3 y_6^2) \end{aligned}$$

Substituting 2 for each of the variables y_1, \dots, y_{15} in

$$\mathcal{Z}_{\text{Aut}_E(K_6)}(y_1, \dots, y_{15})$$

yields 156. \diamond

9.6 GENERAL GRAPHS, DIGRAPHS

With some small variations, the same techniques used to count the isomorphism types of simple graphs can be applied to counting graphs with multiple edges, self-loops, and edge directions.

Counting Multigraphs

DEF: A *multigraph* is a graph model in which multiple edges are permitted, but not self-loops. A *c-multigraph* has at most c edges joining any two vertices.

In counting isom types of simple n -vertex graphs, the model was edge 2-colorings of K_n . The color 1 represented the presence of an edge and the color 0 the absence. If the number of edges between two vertices is permitted to rise from 1 to c , then the number of colors in the model is increased from 2 to $c + 1$.

Proposition 9.6.1. *The 3-vertex 2-multigraphs fall into exactly 10 isomorphism types.*

Proof: The first step is calculating the cycle index

$$Z_{\text{Aut}_V(K_3)}(t_1, t_2, t_3) = \frac{1}{6}(t_1^3 + 3t_1t_2 + 2t_3)$$

The second is transforming it to

$$\mathcal{Z}_{\text{Aut}_E(K_3)}(y_1, y_2, y_3) = \frac{1}{6}(y_1^3 + 3y_1y_2 + 2y_3)$$

The final step of substituting 3 yields

$$\begin{aligned} \mathcal{Z}_{\text{Aut}_E(K_3)}(3, 3, 3) &= \frac{1}{6}(3^3 + 3 \cdot 3 \cdot 3 + 2 \cdot 3) \\ &= \frac{60}{6} = 10 \quad \diamond \end{aligned}$$

The result of Proposition 9.6.1 is confirmed by the list of multigraphs in Figure 9.6.1.

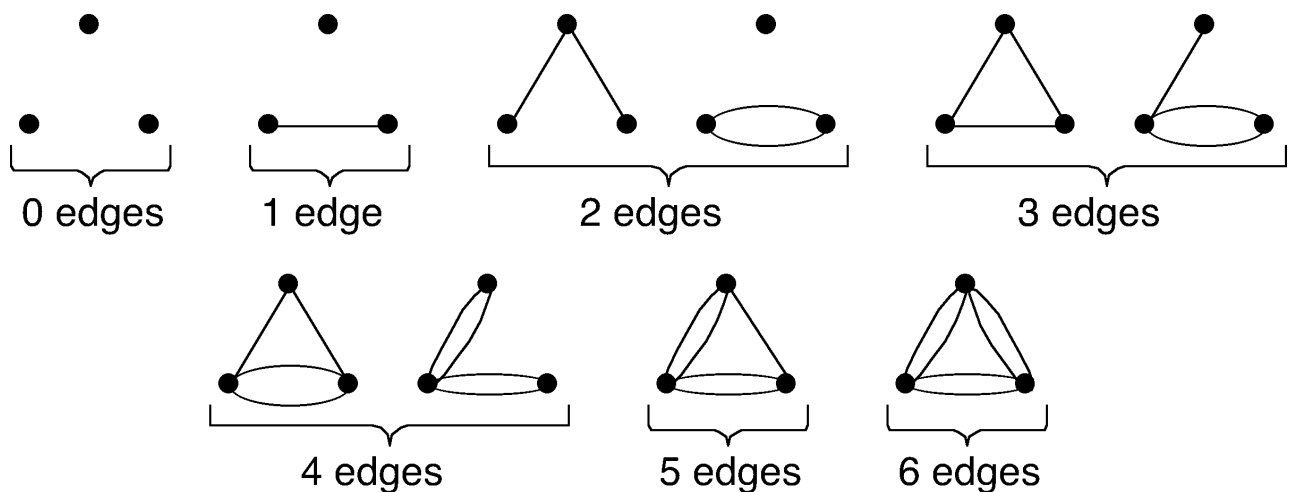


Fig 9.6.1 The ten 3-vertex 2-multigraphs.

Counting General Graphs

Augmenting the complete graph by adding a self-loop at every vertex enables us to solve a counting problem for general graphs.

DEF: The *very complete graph* K_n° on n vertices has an edge joining each pair of vertices and a self-loop at each vertex.

The cycle index for $\mathcal{A}ut_V(K_n^\circ)$ is the same as for $\mathcal{A}ut_V(K_n)$. However there is a slightly different rule for transforming a cycle structure. Whatever cycle structure would have been obtained for $\mathcal{A}ut_E(K_n)$ is augmented by a factor of y_j for each factor t_j .

Prop 9.6.2. *There are exactly 20 isomorphism types of 3-vertex general graph with edge multiplicity at most 1.*

Proof: Under the modified transformation rule, the cycle index

$$Z_{\mathcal{A}ut_V(K_3^\circ)}(t_1, t_2, t_3) = \frac{1}{6}(t_1^3 + 3t_1t_2 + 2t_3)$$

is transformed into

$$Z_{\mathcal{A}ut_E(K_3^\circ)}(y_1, y_2, y_3) = \frac{1}{6}(y_1^6 + 3y_1^2y_2^2 + 2y_3^2)$$

Substituting 2 yields

$$\begin{aligned} Z_{\mathcal{A}ut_E(K_3^\circ)}(2, 2, 2) &= \frac{1}{6}(2^6 + 3 \cdot 2^2 \cdot 2^2 + 2 \cdot 2^2) \\ &= \frac{120}{6} = 20 \quad \diamond \end{aligned}$$

Figure 9.6.2 shows the isomorphism types for 0 to 3 edges. The graphs with 4, 5, and 6 edges are the complements in K_n° of the graphs with 2, 1, and 0 edges, respectively.

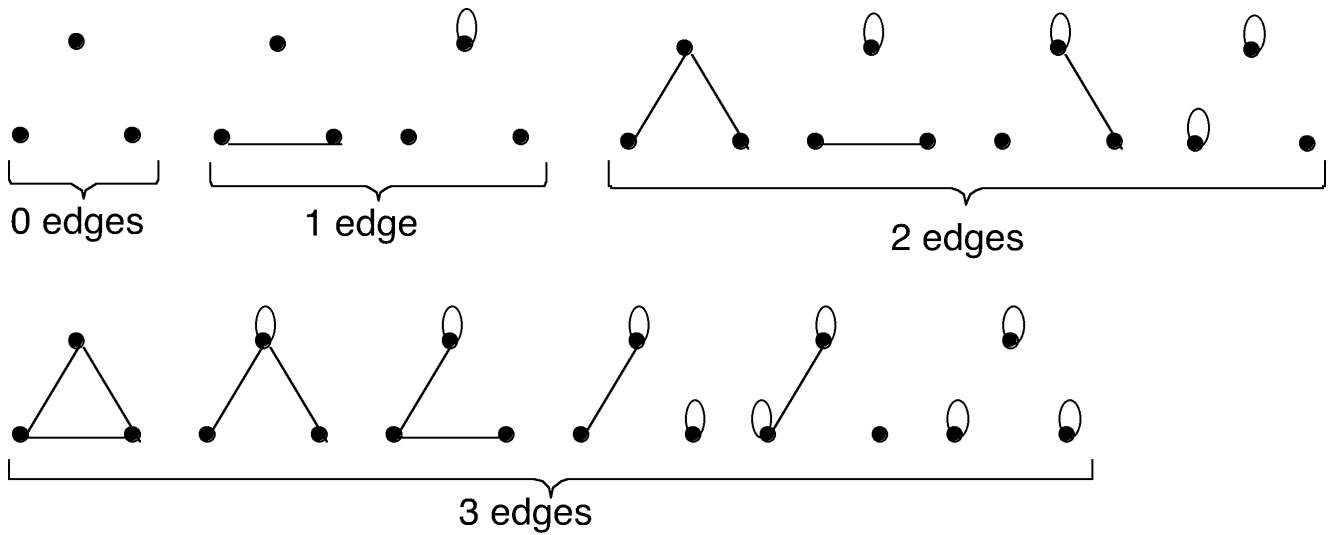


Fig 9.6.2 The 3-vertex general graphs with edge multiplicity at most 1 and at most 3 edges.

Counting Simple Digraphs

Another modification of the main model enables us to count isomorphism types of digraphs.

DEF: The *complete digraph* \vec{K}_n has n vertices and an arc from each vertex to each other vertex.

The cycle index for $\text{Aut}_V(\vec{K}_n)$ is exactly the same as for $\text{Aut}_V(K_n)$. However there are different rules for transforming a cycle structure, as follows.

Thm 9.6.3. *Let π be an automorphism of the complete digraph \vec{K}_n , represented by permutations π_V on $V_{\vec{K}_n}$ and π_E on $E_{\vec{K}_n}$. Then*

- (i) $t_{2p+1} \rightarrow y_{2p+1}^{2p}$: Each $(2p+1)$ -cycle in π_V corresponds to $2p$ $(2p+1)$ -cycles in π_E .
- (ii) $t_{2p} \rightarrow y_{2p}^{2p-1}$: Each $(2p)$ -cycle in π_V corresponds to $2p-1$ $(2p)$ -cycles in π_E .
- (iii) $t_p t_q \rightarrow y_{\text{lcm}(p,q)}^{2\text{gcd}(p,q)}$: Each $(p$ -cycle, q -cycle)-pair in π_V , with $p \neq q$, corresponds to $2\text{gcd}(p,q)$ $\text{lcm}(p,q)$ -cycles in π_E .
- (iv) $t_p t_p \rightarrow y_p^{2p}$: Each pair of p -cycles in π_V corresponds to $2p$ p -cycles in π_E .

Proof: Omitted. Analogous to the proof of Theorem 9.5.5. ◇

Proposition 9.6.4. *There are exactly 16 isomorphism types of 3-vertex simple digraph.*

Proof: Under Theorem 9.6.3, the cycle index

$$Z_{\text{Aut}_V(\vec{K}_3)}(t_1, t_2, t_3) = \frac{1}{6}(t_1^3 + 3t_1t_2 + 2t_3)$$

is transformed into

$$Z_{\text{Aut}_E(\vec{K}_3)}(y_1, y_2, y_3) = \frac{1}{6}(y_1^6 + 3y_2^3 + 2y_3^2)$$

Substituting 2 yields

$$\begin{aligned} Z_{\text{Aut}_E(\vec{K}_3)}(2, 2, 2) &= \frac{1}{6}(2^6 + 3 \cdot 2^3 + 2 \cdot 2^2) \\ &= \frac{96}{6} = 16 \end{aligned} \quad \diamond$$

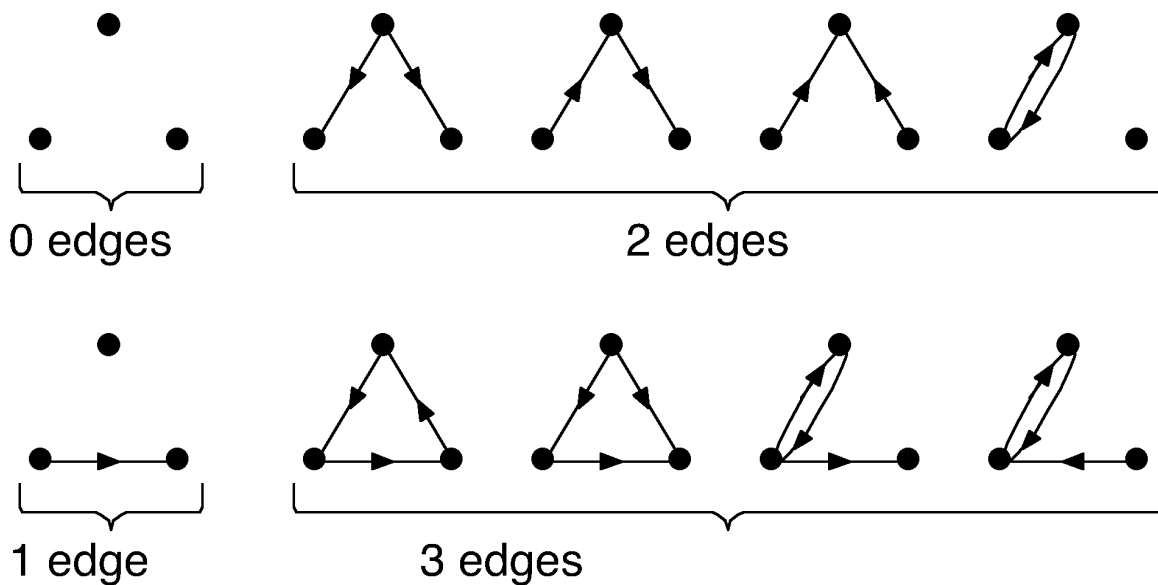


Fig 9.6.3 The 3-vertex simple digraphs with at most 3 edges.